1

Introduction to Ceramic Materials

Laura Treccani

CSMT Gestione S.c.a.r.l., Polo Tecnologico – Innovative Contamination HUB, Via Branze 45, 25123 Brescia, Italy

1.1 Introduction: Ceramics for Biotechnological and Environmental Applications

Ceramic materials have been a part of human life for close to 30 000 years, and because of their superior properties, functionalities, and aesthetic characteristics, have become indispensable for a wide range of technical applications, consumer products, and everyday items [1].

Ceramics were the first man-made materials [2], and they played a very important role until about 1500 C.E., when metal technology took over (Figure 1.1). A second ceramic age started in the mid-twentieth century that witnessed the development and use of "new advanced ceramics," overcoming age-old limitations, such as poor mechanical strength and brittleness [1, 4]. A fast technical evolution supported by innovative processing methods enabled the development of multifunctional and smart materials with outstanding characteristics and opened new unimaginable possibilities. This has gone along with new approaches and prospective in material design and, generally speaking, there has been a shift from "homogeneity to controlled inhomogeneity." As the environments where materials are used become more complex, demanding, and severe, there are frequent cases in which the conventional homogeneous ceramics are inadequate and defective. "Inhomogeneous materials," or more precisely functionally graded materials, are characterized by smooth varying structure or composition. This means that their properties change continuously, and different characteristics can be achieved on separate surfaces, layers or parts. A gradation of properties across the volume, performing a set of specific and diverse functions within the given material, overcomes the inherent limit of homogeneous ceramics and leads to highly customizable multifunctional materials (see, e.g. Chapter 16 "Functionally Graded Materials" in [5]).

Now, the importance of ceramics is stronger than ever, and global trends show that different ceramics with multiple functionalities, along with sustainable, long-term innovative technologies, are tackling some of the major global challenges such as healthcare, environmental pollution, and energy shortages among others. For the sake of completeness, it must be stated that the production volume of advanced ceramics falls strongly behind that of the

Surface-Functionalized Ceramics: For Biotechnological and Environmental Applications, First Edition.
Edited by Laura Treccani and Fabian Meder.

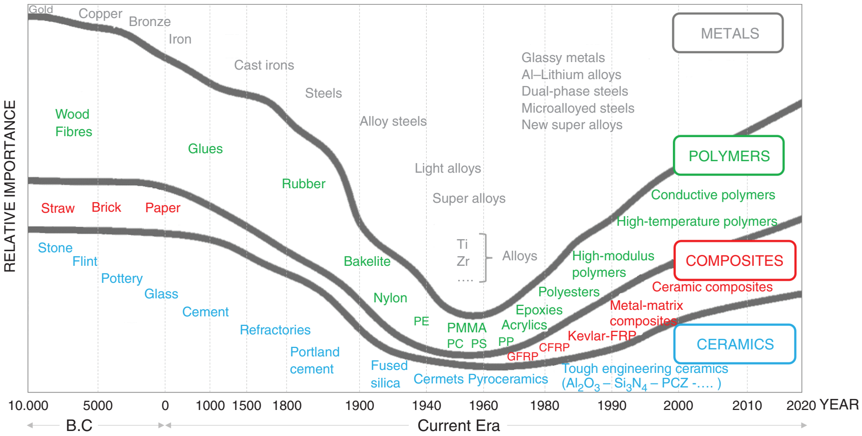

Figure 1.1 Historical timeline of development of materials. Source: Adapted from Ashby et al. [3].

classic ceramics (bricks, tiles, cement/concrete, etc.), but owing to their high value-added nature, their sales volume approaches those of the classic ceramics [1].

In comparison to other materials, ceramics feature unique structural and functional properties and are well suited to being combined with other materials. This makes them the ideal choice for long-life components for thermally, mechanically, and chemically demanding applications, such as chemical and pharmaceutical processes, biomedicine, environmental monitoring, remediation, and food processing.

Examples of the application of ceramics to relevant technical fields are here briefly introduced. Ceramic membranes were developed more than 30 years ago and are becoming an important technology in the emerging areas of separation, purification, and water management for the upstream oil and gas industry, as well as in refineries [6–13]. Ceramic membranes outdo their polymeric counterparts because of their capacity to withstand harsh operating conditions in terms of pH, temperature, pressure, and chemical stability. These peculiarities make ceramic membranes usable several times without any loss in performance. Therefore, they can be considered potential candidates for targeting worldwide goals aimed at improving environmental remediation, alternative energy, and raw material-saving. Ceramic membranes are easy to clean and sterilize, and they can contribute to the production of high-quality foods as well as chemical and pharmaceutical compounds, thus allowing this industrial sector to satisfy more demanding quality standards. This makes them suitable for filtration of biological fluids, foodstuff and water purification, recovery and recycling of organic solvents, dye separation, filtration of acids and caustics, and so on [8, 14]. Ceramic membranes represent an inexpensive option for building microbial fuel cells (MFCs), a highly promising technology to produce electricity, and these can be used to treat wastewater [15]. Ceramic membranes are proposed as suitable candidates for the purification and recycling of chemicals like boric acid from radioactive waste water, thus reducing the emission of radioactive wastewater as well as enabling the reuse of high-value ^{10}B-rich nuclear-grade boric acid from nuclear power plants [16]. Ceramic filters can be effectively employed to reduce gaseous and volatile organic compound (VOC) emissions from industrial complexes and foster the Clean Air Act, implemented and enforced by the Environmental Protection Agency (EPA), to safeguard public from exposure to harmful toxic gases [17]. Different forms of ceramics are widely used for air quality, environmental protection and fight climate change [18], by e.g. capturing or decomposing particulate matter (PM), nitrogen oxides (NO_X), and other VOC, which are mainly responsible for heavy pollution. A striking example is titania, which is largely used in photocatalytic, self-cleaning, and "antipollution" systems [19]. Continuous growth of the global ceramic filter market is expected because of more stringent environmental regulations in developed and developing countries with regards to water management (both drinking and disposal water) and air quality. However, some issues regarding performance and manufacturing costs still need to be overcome to meet the economic feasibility.

Another area where ceramic materials are widely used is in sensing and monitoring. Ceramics are considered a high-potential alternative to silicon for the fabrication of thick films for microelectromechanical systems (MEMS) and microdevices [20, 21]. Ceramic sensors feature mechanical strength and resistance to chemicals, and they are thermally and physically stable in hostile liquid or gaseous environments. MEMS devices are used in different sectors, such as automotive, aerospace, medical, industrial process control, instrumentation, and telecommunications for products such as airbag crash sensors, pressure sensors, biosensors and ink jet printer heads [20], humidity sensors [22], and high-temperature sensors [23]. For example, negative temperature coefficient of resistance (NTCR) ceramic sensors occupy a respected market position because they afford the best sensitivity and accuracy at the lowest price [24].

These examples illustrate, indeed, only some of the application potential of ceramics for biotechnological and environmental purposes. Due to the rapidly changing technological, environmental, social, and industrial trends and requirements, a constant increase in the demand for customized, unconventional materials exists. In response to the changing needs, several approaches have been pursued to create or add and combine new functionalities in materials. A particularly important approach is surface functionalization, which can be roughly defined as the modification of the surface by physical, chemical, or biological methods, or a combination of them. New characteristics can be given to the surface, which can largely differ from the original one. Surface functionalization is extremely versatile and can be applied to particles, thick and thin films, or bulky parts with varying compositions.

The choice of a particular material and a functionalization strategy is a rather delicate issue. Not only the properties of the single components must be considered but also their interaction, the whole manufacturing process, and the final application setting (e.g. chemical and environmental conditions). Functionalized oxide and nonoxide ceramics have been developed and contributed to revolutionizing many technical sectors as well as everyday life. For example, by wet chemistry approaches, also known as *chimie douce*, organic and inorganic components can be brought together and offer new opportunities for the scientist's imagination and the synthesis of innovative, multifunctional hybrid, or bioinspired materials. Surface functionalization can be achieved by other methods, for example, based on physical approaches, and these are not less important. Despite this, the scientific and industrial communities are still actively working to develop innovative and better performing materials and developing strategies for the design of new materials, characterization, and understanding of their structure and properties. Surface functionalization will be thoroughly treated in Chapter 3.

In this chapter, a general definition of ceramics is given, and their main features will be described. In addition, the main application fields of ceramic materials together with some examples, with a main focus on biotechnological and environmental purposes, will be introduced. Some of the most relevant advanced ceramic materials for these applications, which are later described in the following chapters, will be highlighted.

1.2 What are Ceramic Materials?

In material science, materials are commonly divided into three primary classes: ceramics, metals, and polymers. This classical designation is based on the types of atoms involved and the bonding between them. The other two widely recognized classes are semiconductors and composites. Composites are combinations of more than one primary material class and often consist of ceramics. Semiconductors are materials with intriguing electrical properties, and most of them are classified as ceramics.

The concept of ceramics derives from the Greek term, $\kappa\varepsilon\rho\alpha\mu o\sigma$, and it is historically related to terracotta and pottery [25]. Ceramics have so profoundly evolved over time, and today's advanced ceramics bear little resemblance to their origins, which makes it difficult to provide a unique and straightforward definition. Perhaps, the most widely accepted definition of ceramics is that "ceramics are nonmetallic inorganic solids" [26]. However, this definition is limiting it provides little information about chemical composition, the nature of bonding forces, or structure and it does not reveal other important properties [27]. For each application, e.g. semiconductor packages, fuel cells, gas sensors, laser host materials, piezoelectric ceramics, electronic devices, biomaterials, filters and adsorbents, sensors, machining tools, and rocketry parts, ceramic materials have very diverse chemical and physical characteristics, which are unique and specifically designed for a particular function [5, 28, 29].

1.2.1 Advanced and Traditional Ceramics

For the sake of completeness, *some* standard *definitions* of set terminology are here briefly introduced. Ceramics can be divided into two major categories: traditional and advanced, which have very diverse applicative sectors as schematically shown in Figure 1.2.

Traditional ceramics can be considered the oldest ceramics, having developed since the earliest civilizations. These are based almost exclusively on naturally occurring raw materials, most commonly silicaceous minerals such as clay, mica, quartz, and feldspars. The term traditional could be misleading, and it must not be associated with low technology. Today, advanced manufacturing techniques, complex tooling, and computer-assisted processes are often used for the manufacturing of traditional ceramics. Evolution is pushed by several new requirements, such as customized technical properties, known and defined chemical and physical characteristics, and low contaminant amounts. Nowadays, traditional ceramics are largely employed for high-volume items such as construction products (bricks and

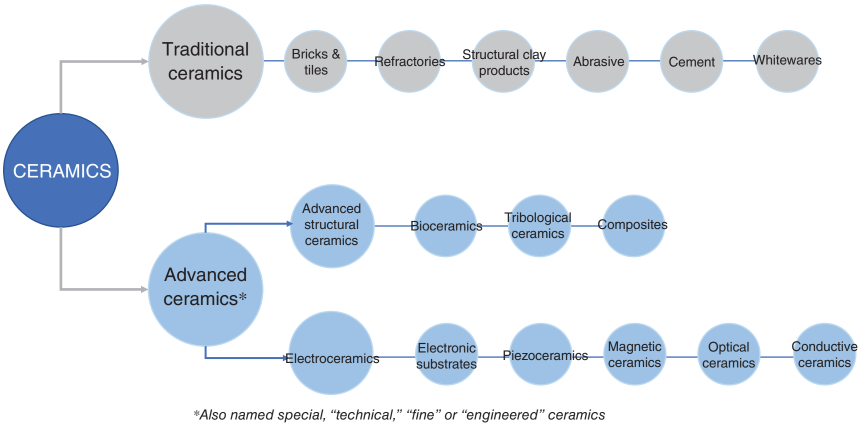

Figure 1.2 Traditional and advanced ceramics: classification and applications. Source: Adapted from Tanzi et al. [30].

tiles, clay-based refractories, cements and concretes, and glasses) and consumer products (whitewares and pottery). Traditional ceramics share the largest proportion of ceramic sales worldwide, and the market is clearly dominated by glass, for example, glass window production [25, 28].

Advanced ceramics have been developed more recently, approximately within the last 100 years, and are also referred to as "special," "technical," "fine," or "engineered" ceramics. The terminology for defining this type of ceramic differs from continent to continent. For example, "advanced" or "technical" ceramics are used in American literature, and "fine" ceramics are used in Japanese literature. The term "technical" ceramics is more frequent in the European context. A further classification, common in the UK, is related to use. Functional ceramics refer to electronic applications, whereas structural ceramics typically refer to mechanically loaded components. According to ISO 20507:2014, these can be described as "materials produced with precisely controlled chemical compositions, microstructures, configurations, and production processes to fulfill intended functions and which are composed mainly of nonmetallic, inorganic substances." In comparison to traditional ceramics, these exhibit superior and very diverse properties and are included in electrical, magnetic, electronic, and optical applications (sometimes referred to as *functional ceramics*) and ceramics for structural applications at ambient as well as at elevated temperatures (*structural ceramics*). Advanced ceramics typically consist of metals and nonmetals and form different classes, such as oxides, nitrides, carbides, and silicides. Other materials can be classified as ceramics. For example, glasses are a special type of ceramic. Glass-ceramics, which can be produced through the controlled crystallization of base glass (known as "ceramming"), share many properties of both glasses and ceramics. Forms of carbon, like diamond and graphite, and all inorganic semiconductors can be considered ceramics [25]. Diamond is an example of elementary ceramic, and it is often used as a reinforcing component. More recently, dispersed primary diamond particles (e.g. detonation nanodiamonds) have been considered for several attractive applications like nanospacer lubrication in water, fluorescent bioprobes, drug-delivery systems, and catalyst carriers [31]. Further information about carbonaceous ceramics will be given in Section 1.5, and its potential for antibacterial applications will be discussed in *Chapter 9*.

1.2.2 Properties of Advanced Ceramics

Advanced ceramics are known for their outstanding properties, such as high melting points, electric insulation, and transparency in the visible range, which are imparted by the ionic–covalent bonds, poor thermal and electrical conductivity due to the tied up valence electrons in bonds, which are not free like in metals; brittleness because of the ionic–covalent bonds; high degree of hardness; and high moduli of elasticity [5, 25, 28, 29].

However, this lists the most common properties of ceramics, and it gives only a relatively simple and limited categorization. Ceramic materials are more complex and do not have uniform characteristics or behaviors, although there are several exceptions. A striking feature of ceramic materials is their possibility to form different types of chemical bonds, including ionic, covalent, and metallic (Figure 1.3).

For example, some ceramics are semiconducting, like barium titanate ($BaTiO_3$), or superconductive like cuprates ($YBa_2Cu_3O_7$), titanates ($SrTiO_3$), or $BaPbO_3$ [5, 25]. Diamond is the best thermal conductor at ambient temperature, and certain ceramics (AlN, BeO, or SiC) perform better than metals like copper. Most ceramics are brittle at room temperature but not necessarily at elevated temperatures. For example, at high temperatures, glass behaves as a viscous liquid and no longer in a brittle manner [25]. The chemical inertness of ceramics is usually taken for granted; however, it can severely differ when ceramics are used at high temperatures, as in the chemical and metallurgical industries [28]. Oxides are stable in oxidizing atmospheres, but nonoxidic ceramics can oxidize even at relatively low temperatures. Silicon compounds (e.g. silicon carbide and silicon nitride) can self-protect from oxidation at high temperatures thanks to the formation of a silica layer [32]. Graphite and carbon compounds are ultrarefractory, but they can only be used in a protective environment. Magnesium oxide and aluminum carbide are unstable in the presence of moisture.

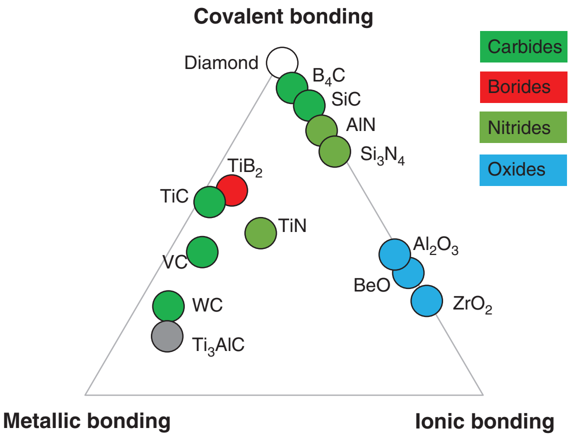

Figure 1.3 Types of chemical bonding of different ceramic materials. Source: Adapted from Heimann [1].

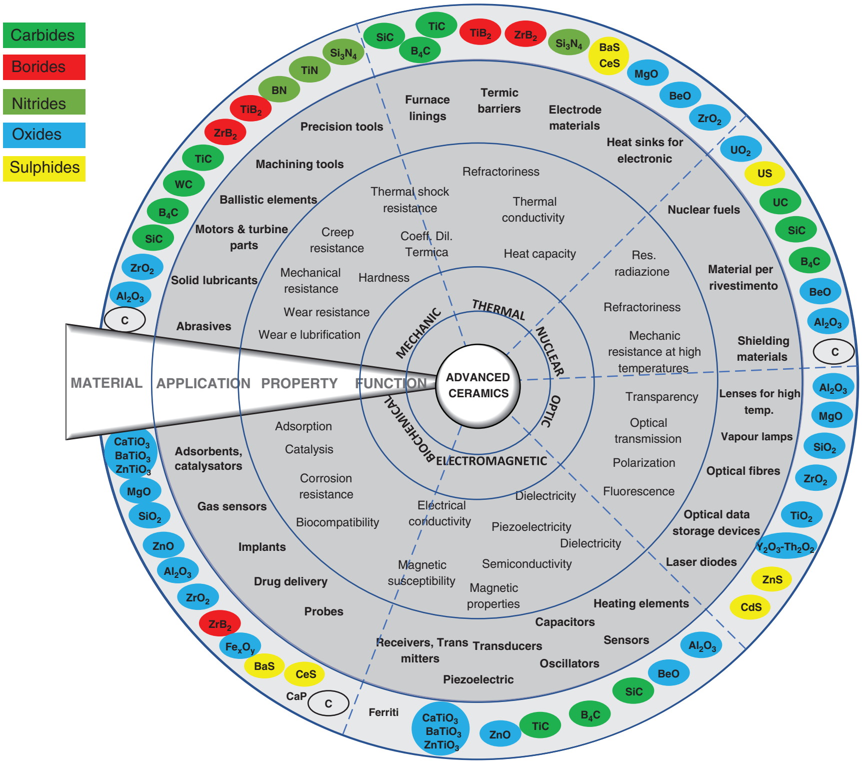

Figure 1.4 Overview of the most relevant advanced ceramics: properties and applications.

In Figure 1.4, an overview of the most relevant advanced ceramics, properties and applications is given. Usually, for a given application, one property may be of particular importance, but in fact, all relevant properties need to be considered [28].

From this point onwards, some general properties of the most relevant ceramic materials for biotechnological and environmental applications and materials considered in other chapters are briefly described. For more exhaustive information that goes beyond the scope of this book, some selected references will be highlighted.

1.3 Oxide Ceramics

All oxides that can be formed from the periodic table elements belong to ceramic materials. Oxide materials provide a plethora of possible applications and offer ample opportunity for different applications, including biotechnology, biomedicine, and environmental purposes (e.g. remediation, monitoring, and energy harvesting).

1.3.1 Alumina

Aluminum oxide, generally referred to as alumina (Al_2O_3), is one of the most important technical ceramic materials, both pure or as a component, and perhaps the most mature high-technology ceramic in terms of quantity produced and variety of industrial uses [29].

1.3.1.1 Alumina Structure and Properties

Alumina features an excellent combination of intrinsic properties and versatility: high melting point (>2000 °C), hardness, strength, abrasion resistance, high electrical resistance, excellent optical properties, chemical stability, and inertness.

Alumina is the only oxide formed by the metal aluminum and occurs in nature as the mineral corundum (Al_2O_3), with several metastable forms, and numerous hydrated phases. There are three trihydroxide forms of aluminum: bayerite [α-Al(OH)], nordstrandite [β-$Al(OH)_3$], and gibbsite or hydrargillite [γ-Al(OH)]. Bauxite is an impure form of gibbsite containing 40–60% of equivalent alumina in the form of hydrargillite, boehmite, diaspore, and silicoaluminous minerals; 10–20% iron oxide; and approximately 5% quartz sand and other various impurities. The two oxyhydroxides are: diaspore (α-AlOOH) and boehmite (γ-AlOOH) [33, 34].

At all temperatures and up to at least 78 GPa pressure, corundum or α-Al_2O_3 is the most stable phase of alumina. The considerably high enthalpy of formation (~1600 kJ/mol[1]) makes alumina one of the most tightly bonded compounds, resulting in very high hardness (9 on the Mohs hardness scale) and high melting and boiling temperatures (2050 and 3500 °C, respectively). The density of corundum is close to 4 g/cm^3, and in single-crystal form, corundum is a bright white solid [26]. Trace amounts of impurities, such as iron, titanium, chromium, copper, or magnesium, can give corundum blue, yellow, pink, purple, orange, or greenish colors [25]. Corundum has a crystal structure consisting of oxygen ions in a slightly distorted close-packed hexagonal (rhombohedral) lattice (space group *R3c*). The aluminum ions occupy two-thirds of the octahedral sites in the oxygen lattice. Alumina has many metastable polymorphs, which are generally divided into two structural categories depending on the O anion arrangement. Metastable aluminas, which are all less dense than corundum, have O packings that are near to close-packed cubic. Eta or gamma aluminas are typically formed at low temperature, and as temperatures rise, alumina transforms in the sequence $\gamma \rightarrow \delta \rightarrow \theta \rightarrow \alpha$ alumina (Figure 1.5) [33, 36]. α-Al_2O_3 is usually prepared as medium–low surface area powder by thermal decomposition of diaspore (α-AlOOH) at temperatures above 450 °C or by calcination of gibbsite ($Al(OH)_3$) at ~1000 °C [36]. Many other variants are also possible. For example, γ-Al_2O_3 can form at higher temperatures and transform directly to α. The kinetics of transformation and the sequence of phases are influenced by several factors, like particle size, heating rate, impurities, and atmosphere. At temperatures above 1200 °C, only the α phase is typically present. At relatively low temperatures (nearly 300 °C), alumina hydrates decompose to Al_2O_3 and water [34].

Alumina in the α and γ forms is a common choice as a catalyst carrier, and corundum is highly important in mineral processing and adsorption of heavy metal elements [33].

Gamma-Al_2O_3 becomes especially advantageous when it is relatively stable against $\gamma \rightarrow \alpha$ conversion, and among all polymorphs, it is the most important for applications, such as catalysts, adsorbents, or coatings [33, 34]. Purities and grain sizes can vary considerably from one product to another. Typically, fine powders, with a grain size of about one micrometer

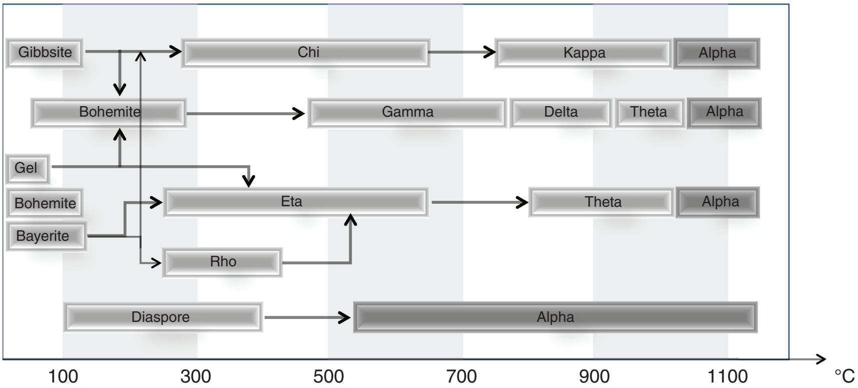

Figure 1.5 Thermal transformation sequence of hydrated alumina. Source: Adapted from Wefers and Misra [35].

and “reactive” powders, like low-temperature-calcined alumina, are necessary to produce sintered parts [34, 37]. An increase in the calcination temperature increases the particle and crystal sizes, which disadvantages the sintering process. For example, reductions in the average particle size, tighter control of its distribution, and improved purity characteristics have been highly beneficial in obtaining finer microstructures in alumina implants and thus better performance [38]. Refractory materials require coarse grains (several hundred micrometers) to limit creep and reduce reactions with the environment, and therefore prefer tabular alumina. It must be noted that alumina reactivity is crucial for many applications, requiring highly densified ceramics with a well-controlled microstructure obtained at sintering temperatures as low as possible [37].

The structures of all forms of alumina (stable, unstable, and hydrated) are listed in Table 1.1.

The Al_2O_3 surface is positively charged at pH 7 because of the alkaline isoelectric point (IEP). The IEP, or the pH where the ξ-potential is zero, of alumina is 8–9 [28, 39, 40]. Alumina solubility in water is finite and depends on the type of solution species, solution pH, temperature, other ionic species, and the solid phase. Generally, alumina is stable in an aqueous environment between pH values of 3 and 12, where Al^{3+} and AlO^{2-} ion release concentrations sum up to a value smaller than 10^{-2} mol l^{-1}. Alumina has a low solubility in solutions with pH ranging from 4 to 9; at 25 °C, it is less than 10^{-7} mol^{-1} at pH 6, but it dissolves readily in strong acids (HCl, HNO_3, H_2SO_4) and strong bases (NaOH, KOH) at temperatures well above ambient (e.g. >90 °C). Solubility, generally, increases with temperature, as it is common for most materials. Alpha-Al_2O_3 is much less reactive than γ-Al_2O_3, but it dissolves in heated alkaline media or eutectics with low melting points. Highly reactive metals (calcium or magnesium) can reduce alumina beyond ~900 °C. Transition aluminas (γ-Al_2O_3), with a metastable structure and very high specific surface area, are soluble in aqueous, acid, or basic solutions but not in neutral aqueous solutions, thus being regarded as an amphoteric oxide [33, 41]. The catalytic activity of transitional aluminas (γ -, η-, δ-, θ-Al_2O_3) is undoubtedly mostly related to the Lewis acidity of a small number of low-coordination surface aluminum ions, as well as to the high ionicity of the

Table 1.1 Crystal structure and physicochemical properties of aluminas.

		Lattice parameters (Angstrom/angle)			
Designation	**Structure**	***A***	***b***	***c***	**Density (g/cm^3)**
Corundum (alpha)	Hexagonal (rhombohedral)	4.758		12.991	3.96
Eta	Cubic (spinel)	7.90			
Gamma	Tetragonal	7.95		7.79	3.2
Delta	Tetragonal	7.97		23.47	3.2
Theta	Monoclinic	5.63	2.95	11.86/103° 42′	3.56
Kappa	Orthorhombic	8.49	12.73	13.39	3.3
α-Al(OH)$_3$ gibbsite	Monoclinic	8.64	5.07	9.72/85°26′	2.42
AlOOH diaspora	Orthorhombic	4.40	9.43	2.84	3.44
α-AlOOH bohemite	Orthorhombic	2.87	12.23	3.70	3.01
β-Al(OH)$_3$ Bayerite	Monoclinic	4.72	8.64	5.06/90°7′	2.53

Adapted from Ganguli and Chatterjee [34].

surface Al—O bond. Characterization studies determined that the transition aluminas also present significant surface basicity. In fact, CO$_2$ adsorption sites on γ-Al$_2$O$_3$ are quite strong, although the density of sites for strong adsorption ($\Delta H \sim 50$–180 kJ/mol) is small (0.06 site/nm^2) [36].

1.3.1.2 Applications of Alumina: Some Examples

Alumina can be considered the foremost basic compound for "advanced ceramics" because it exhibits exceptional versatility. Applications include: high-temperature systems; catalyst substrates; filters; biomedical implants; optical systems; abrasive materials; bearings; cutting tools; electrical insulators; refractory materials; jewelry; filler for plastics and toothpaste; desiccant; and a wide variety of other industrial products [25, 33, 42–45]. Pressed powders are employed in electrical insulators, windows or radomes transparent to microwaves, envelopes for lamps, and electrical devices [5, 28]. As a single crystal, it is used for optical purposes, electronic applications (e.g. as a semiconductor), in watch bearings, and pressure-resistant windows. Polycrystalline alumina is the basis of refractory bricks, crucibles, sparkplug insulators, and biomedical implants [25, 26]. Alumina is the first choice for the ball joint in a hip prosthesis, owing to its hardness and characteristic low friction [25, 46]. Porous alumina membranes are used for medical treatments [47], wastewater treatment, energy and environmental remediation [48], and other applications [49]. Additionally, alumina is used as a component in ceramics and glasses, mullite components, electrical insulators, porcelain, and durable glasses.

Pure alumina has been used for nearly 20 years in dental and orthopedic applications, and in addition to its advantageous chemical and mechanical properties, it exhibits excellent biological tolerance (allergy-free and biocompatible), an absence of wear, and the rarity of osteolysis. Alumina is mostly used as the bearing surface in total hip joint endoprostheses [50, 51]. The usage of alumina for dental applications is limited to abutment materials because of its lower fracture toughness and bending strength compared with zirconia [40]. To overcome the limitation, a new material consisting of alumina doped with polycrystalline metastable tetragonal yttria–partially stabilized zirconia has been developed, and it is currently being exploited for femoral heads for the hip endoprosthesis. Such materials have outstanding mechanical properties, like high fracture strength greater than 700 MPa and fracture toughness up to 12 $\text{MPa m}^{1/2}$. In this material, cracks introduced by external loads tend to move toward the zirconia particle aggregates; the crack energy will force the transformation toughening of tetragonal zirconia into monoclinic zirconia [52]. This mechanism will be described later in the section dedicated to zirconia.

Alumina finds large usage as a stationary phase in chromatography. The activity of alumina is affected by two main factors, namely the chemical nature of the surface, which involves the number of hydroxyl groups and acid sites on the surface, as well as the texture of the solid, and the availability of various reactants to reach an active site, which depends on the pore sizes and their distribution. Particular advantages are high selectivity, thermal stability, and resistance to different external factors [53]. Columns packed with alumina combined with anion-exchange columns can be used for the determination of sulfate in brines and biological fluids and for the trace determination of iodide down to the low ppb range in mineral waters and fruit juice samples. Alumina proved to be a highly selective stationary phase for the preconcentration of sulphate from complex matrices. Thanks to its selectivity, it is well suited for online column-coupling techniques [54].

Other well-known applications of alumina are in drug-delivery systems [55, 56] and medical biosensing devices [57]. Alumina membranes features porous structures, large surface area, tunable pore size and pore size distribution, low fabrication costs, and ease of processing [40]. Alumina membranes are extensively used for protein separation and purification because of their moderate hydrophilic character (contact angle of 40–50°) and the lowest cost among other oxide materials. One of the main concerns about the applications of alumina membranes and other ceramics is membrane fouling, which occurs because of the deposition and adsorption of proteins or other biological species on the surface and pore walls. Extensive work is aimed at minimizing membrane fouling using several approaches, like enhancing the hydrophilic character of the membranes [58], creating a coating of SiO_2 by sol–gel [59], or well-organized mesoporous TiO_2 layers on poly(vinyl pyrrolidone) precoated porous support [60], as well as linking bactericidal silver nanoparticles encapsulated in positively charged polyethyleneimine [61]. Surface functionalization with organic modifiers has been widely applied to enhance long-term stability and operability, as well as to control biomolecule adsorption and release [40].

Sensor devices based on Al_2O_3 are excellent sensing materials for humidity. These devices operate at near room temperature and show good stability, as no surface chemical reactions take place when exposed; they have a relatively long service time and can be regenerated. Moreover, in comparison to other humidity-sensing materials, devices based on Al_2O_3 show a very rapid response time of the order of one minute. Al_2O_3-based sensors are volume effect devices, whereas the porous Al_2O_3 film acts as a dielectric with pores whose conductivity varies as a function of moisture content trapped in micropores [62]. At relative higher temperatures (about 450 °C), aluminum oxide-based sensors can detect different gases like H_2,

O_2, and CO_2 [62]. Theoretical calculations of gas adsorptions on α-Al_2O_3 (0001) surface indicate that the adsorption of a monolayer of —OH on top of the surface aluminum ions and hydrogen atoms bonded to the surface oxygen ions generates a new bond that is shifted a few eV above the top of the valence band in the bulk bandgap [62]. Nanoporous alumina films can be used as moisture sensors for the detection and discrimination of several cyclic VOC like cyclohexanes, cyclohexene, benzene, toluene, and xylene isomers [63].

1.3.2 Titania

Titanium dioxide (TiO_2), also known as titanium (IV) oxide, finds use as a pigment in paints (called Titanium white or Pigment White 6), coatings, cosmetics, foodstuff, dye-sensitized solar cells, self-cleaning windows, whose production is affected by gross domestic product worldwide [64–67]. The first industrial production of TiO_2 dates back to 1918. Now, several megatons of TiO_2 are produced per year by precipitation from oversaturated solutions according to the sulfate process, by hydrolysis or pyrolysis of titanium tetrachloride, or by several other, highly sophisticated methods [67]. In the recent decades, particular attention has been given to nanoscale titania because of its photocatalytic properties, which have found a great number of applications in many areas such as material science, physics, biology, chemistry, and medicine. Nanoscale titania is now available in different forms, including spheroidal crystallites and particles, along with tubes, sheets, and fibers. When compared with other nanomaterials, it is abundant and potentially of low cost [64].

1.3.2.1 Titania Structure and Properties

Titania exists in three different forms: rutile, anatase, and brookite. Rutile is the thermodynamically stable form within a wide range of temperatures and oxygen partial pressures. Anatase and brookite are metastable and readily transformed to rutile when heated [64]. TiO_2 also exhibits high-pressure forms, including the monoclinic titanium dioxide (B) or TiO_2(B) [64, 68] and the orthorhombic α-PbO_2-like form [69].

Each of the TiO_2 structures consists of Ti cations in the center of the oxygen octahedra. Rutile, anatase, and brookite show a decreasing symmetry (Figure 1.6).

Rutile has tetragonal symmetry, and the structure is constructed by linking octahedra. An octahedron is placed at each of the eight corners such that two actually share an apex. The six points of these octahedra are then connected by one rotated octahedron at the center

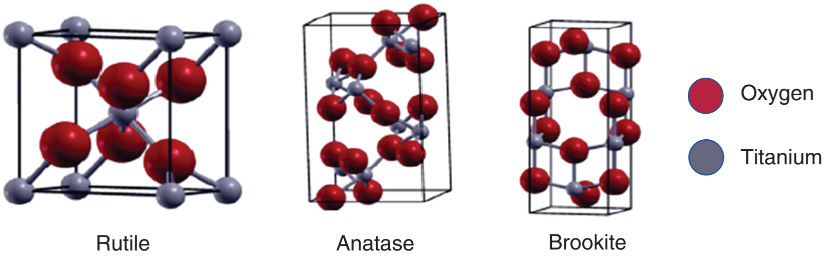

Figure 1.6 Structures of main titania polymorphs (unit cells): rutile, anatase, and brookite. Source: Adapted from Esch et al. [70].

Table 1.2 Structural information and properties of most common titania polymorphs.

Designation	Structure	Lattice parameters (Angstrom) *a*	*b*	*c*	Density (g/cm^3)
Rutile	Tetragonal	4.584		2.953	4.240
Anatase	Tetragonal	3.758		9.514	3.830
Brookite	Orthorhombic	5.456	9.182	5.143	4.170

Carpenter et al. [66]/with permission of Springer Nature.

of the unit cell. The edges of the octahedra are linked together to form chains along the z-axis. Each Ti^{4+} ion is surrounded by six O_2^- anions, and each O_2^- anion is surrounded by three Ti^{4+} ions. The structure is primitive tetragonal, with $a = 0.459$ nm, $c = 0.296$ nm, and two formula units per unit cell (Table 1.2). The rutile structure has been described as a distorted hexagonal close-packed oxide array, alternate rows of octahedral sites are full and empty, and it is regarded as an ionic structure [25, 62, 71, 72]. Rutile is the simplest of the titanates with high dielectric constants (κ) of ~100 and is more thermally stable than anatase [25].

In anatase, the arrangement of the anions and cations is similar, and the crystal is tetragonal. Each octahedron shares four of its edges with other octahedra and is distorted. The conventional unit cell contains four TiO_2 units and 12 atoms. Each O atom is coordinated to three Ti atoms, lying in the same plane in the unrelaxed structure, through one long bond and two short bonds [72].

Brookite has a more complex orthorhombic crystalline structure with octahedra sharing both edges and corners to such an extent so as to give the crystal the correct chemical composition. The octahedra are distorted and present the oxygen atoms in two different positions. The bond lengths between the titanium and oxygen atoms are all different. Oxygen atoms in the octahedron are distributed on the two faces nearly perpendicular to the [73] direction. Every octahedron shares three edges: one of these determines the crystal distribution along the [73] direction, and the other two determine it along the (001) direction [65].

By calcination at high temperatures, brookite is transformed to rutile. The transformation occurs directly or via anatase, depending on several factors, including crystallite size, size distribution, and contact area of the crystallites in the powder [65].

The monoclinic titanium dioxide (B) has a structure that consists of four edges sharing TiO_6 octahedral subunits, and it has a relatively open three-dimensional framework with significant voids and continuous channels. TiO_2(B) performs better than other TiO_2 polymorphs because of these properties. For example, TiO_2(B)-based nanotubes and nanowires have greater performance in rechargeable lithium batteries, and high photocatalytic activity was also observed by using TiO_2 nanostructure with polycrystalline phase containing anatase and TiO_2(B) [64].

In oxidation state +4, titanium forms several hydroxides, and different IEP values ranging from 3 to 8.2 have been reported [74, 75]. Such significant differences and discrepancies in IEP values can be attributed to several factors, including impure materials or erroneous procedures [74] and the specific properties of the analyzed materials, such as nanoscale roughness and surface morphology [76].

The solubility behavior of titania and the water–titania interface have been the subject of many investigations as the state of the surface charge influences many applications [67]. In particular, with the increasing synthesis of nanomaterials, several questions about the stability of nanostructures have been posed [77].

Titania is commonly believed to be insoluble in water and most acids at room temperature. Indeed, depending on the titanium dioxide species, pH, and temperature, the equilibrium solubility is found to be in the range of micro- to nanomoles per liter [67, 77]. In aqueous media ($\text{pH} > 1$) at ambient temperature, crystalline bulk titanium dioxide shows very small equilibrium solubilities that can only be quantified by employing trace analysis [77]. Titania is soluble in hot concentrated sulfuric acid and in alkaline conditions [40, 77, 78].

Among all oxides, titania is the most thoroughly studied d_0 transition metal oxide. TiO_2 is an n-type semiconductor and has received increased attention because of its advantageous properties such as: high dielectric constant, excellent optical transmittance, high refractive index, high chemical stability, and suitable energy bandgap [62]. The most outstanding feature is related to its photocatalytic activity. Investigations into the photocatalysis of titanium dioxide began in the 1950s, but practical applications of TiO_2 as a photocatalyst started in 1972 with the discovery by Fujishima and Honda [79], who reported for the first time the photocatalytic splitting of water on titanium dioxide electrodes [80]. When TiO_2 is irradiated by photons with energy in the near ultra-violet (with $\lambda < 390$ nm), an electron is excited out of its energy level and leaves a hole in the valence band. A schematic representation of this mechanism is given in Figure 1.7.

The promotion of electrons from the valence to the conduction band generates electron–hole pairs (Eq. (1.1):

$$\mathrm{TiO_2} + h\nu \rightarrow \mathrm{e^-} + \mathrm{h^+} \tag{1.1}$$

The valence band (h^+) potential is positive enough to generate hydroxyl radicals ($^{\bullet}OH$) on the TiO_2 surface, and the conduction band (e^-) potential is negative enough to reduce molecular oxygen. The hydroxyl radical is a powerful oxidizing agent, which may attack the organic matters present at or near the surface of TiO_2, and it is capable of degrading toxic and bioresistant compounds into harmless species like H_2O and CO_2 (Figure 1.7). It is generally assumed that the photodegradation rate of anatase is higher than that of rutile; however, this is not always true. Photodegradation depends on the polymorph type and, even to a large extent, by other factors, such as the crystalline state, surface area, and particle size.

1.3.2.2 Applications of Titania: Some Examples

Titania's photoelectrolytic properties have been exploited for the generation of renewable, fossil-fuel-free clean energy with minimal environmental impact. Titania-based materials are considered to be the most promising candidates for photoelectrodes for solar hydrogen as they exhibit outstanding resistance to corrosion and photocorrosion in

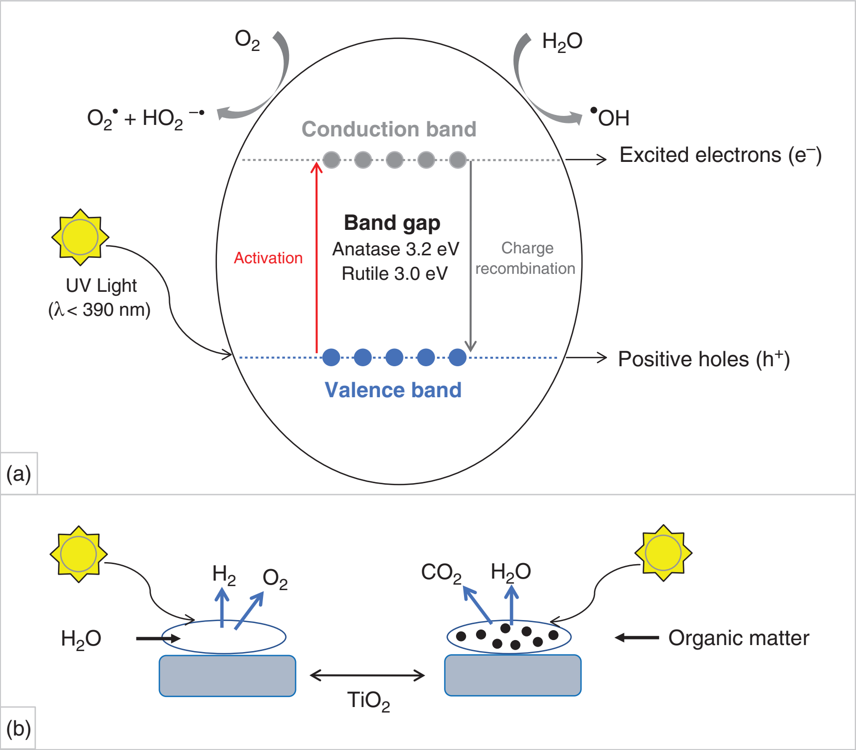

Figure 1.7 (a) Photocatalytic mechanism of titania. (b) Decomposition of gases on titania surfaces. Source: (a) Adapted from Khataee and Mansoori [64], Copyright 2010, with permission from Elsevier. (b) Adapted from Ohama and Van Gemert [79].

aqueous environments, in addition to low cost and low toxicity [69, 79]. However, there are still several critical aspects to be solved for the efficient solar production of hydrogen from the technological point of view. Limitations are represented by the optical band of 3.2 eV, which is much larger than the resonance energy of 1.23 eV required for water splitting, and UV light accounts for only 4% of the solar spectrum compared with 45% visible range. Different approaches have been pursued to improve the efficiency of solar energy-harvesting materials, for example, by shifting the optical response to the visible range [81]. These include doping, co-doping, coupling/composite hybridization, doping and coupling, capping, coating, and so forth. Anionic and cationic compounds, including a wide range of transition metals such as Fe, Pt, Co, Nb, and oxides like RuO_2, have been used for this purpose [82]. Other approaches rely on the integration of light-harvesting proteins and other photosynthetic molecular machineries [83] like hematoporphyrins [84].

Titania has gained great importance in the field of gas sensing because of its surface interactions with reducing or oxidizing gases [85]. With UV photon absorption, an electron–hole pair that can facilitate reduction and oxidation chemistry at the material surface. These redox reactions clean the surface by breaking down organic contaminants to form mainly CO_2 and H_2O molecules (Figure 1.7) [62, 79]. Thanks to this property, TiO_2 (rutile in most cases) is used as a humidity- and pressure-sensitive material and as a gas sensor for H_2, O_2, and CO [62]. It is also used in other sensing applications, such as for the determination of glutamate in water and biological samples [86], chemical discrimination of fresh fruit juices [87], and as an oxygen sensor for the control of air-to-fuel ratio in automobile engines to improve the fuel economy efficiency, and to reduce the harmful emission of gases, such as CO, NO_x, and different hydrocarbon exhausts. Rutile is typically used as it is at a stable phase above 800 °C [62].

Titania-based sensors with enhanced sensitivity for ethanol, methanol vapors, and other specific molecules find applications in food analysis [88], wine identification, electronic noses [89], and breath analyzers [90].

Hydrogen is of particular importance in the medical sector, and it is used as an indicator of different diseases, such as lactose intolerance, fructose malabsorption, microbial activity, bacterial growth, fibromyalgia, diabetic gastroparesis, and neonatal necrotizing enterocolitis. For all these purposes, reliable monitoring with high sensitivity down to a few ppm is demanding. Various types of hydrogen sensor technologies have been developed, such as Schottky junction, fiber optic, catalytic, electrochemical, field effect transistor (FET), oxide semiconductor, and combinations of these. Oxide semiconductor gas sensors are relatively simple and low-cost. They commonly operate at elevated temperatures to enhance gas sensitivities and enable fast and reversible reactions, but such conditions are not favorable for many applications, such as biomedical applications, particularly those requiring low-power operation or involving flammable environments. Some studies report the use of anatase nanotube arrays for highly selective detection of H_2 at low temperatures (<200 °C), in the presence of several reducing gases, including NH_3, CO, and C_2H_5OH, and with a very short response time (<1 second) [91] or H_2 detection at room temperature in the presence of less than or equal to 1000 ppm of H_2 [92].

Since 1990, titania has been exploited as an alternative to silica for HPLC packing because of its high mechanical strength, excellent pH stability, and amphoteric ion exchanger characteristics [93]. Titania has hydroxyl groups on its surface that are only slightly acidic so that native titania can be used to separate basic molecules under normal-phase conditions. An example of titania microspheres used for HPLC packing obtained by the sol–gel method is shown in Figure 1.8. Titania packings can used for e.g. the purification of basic fine chemicals and pharmaceuticals or for the separation of nonbasic isomeric substance mixtures [95]. Capillary titania-based columns offer a compromise between the high permeability and the important loading capacity required for miniaturized sample preparations. Such systems can be, for example, used for the enrichment of nucleotides [96].

1.3.3 Zirconia

Zirconium dioxide (or zirconia: ZrO_2) is another versatile oxide and is widely used for dental and orthopedic implants [73, 97, 98], drug delivery [99–101], chromatography [44, 45], biosensors [102, 103], ionic conduction [104–106], energy harvesting [66, 107], mechanical purposes, or in jewelry. Like alumina, zirconia has excellent biocompatibility but exhibits

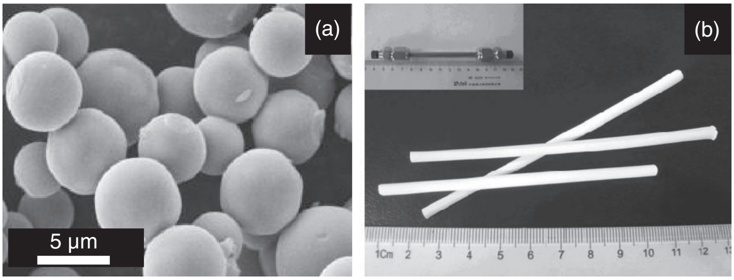

Figure 1.8 (a) Sol–gel porous titania microspheres for HPLC packing. (b) Titania monolith columns for Hydrophilic Interaction Liquid Chromatography (HILIC). Inset: photograph of chromatography column of titania monolith. Source: (a) Du et al. [93]/Reproduced with permission of Elsevier. (b) Wei et al. [94]/Reproduced with permission of Springer Nature.

higher strength and fracture toughness. Often, alumina and zirconia are combined, and the resulting composite (zirconia-toughened alumina, or ZTA) has higher ductility and fracture toughness than each constituent. ZTA is widely used in total hip arthroplasties or other structural applications [108, 109].

1.3.3.1 Zirconia Structure and Properties

Zirconia is found in its natural state in the form of baddeleyite but is more frequently prepared from zirconium silicate sands (zircon: $ZrSiO_2$) or zirconium orthosilicate. Zirconia has a very high melting temperature ($T \sim 2880\,°C$); it solidifies in a cubic phase (c-ZrO_2, group space Fm3m), then transforms ($T < 2370\,°C$) to a tetragonal phase (t-ZrO_2, $P4_2/nmc$), and finally becomes monoclinical (m-ZrO_2, $P2_1/c$). Monoclinic zirconia is stable up to about 1100 °C, and the transformation to the tetragonal phase occurs as the temperature increases to 1200 °C. Such a transformation is accompanied by a volume contraction of 3–5% and is reversible, so that on cooling from 1000 to 850 °C, there is a similar volume increase. Such volume change results in the formation of large shear strains, and thus, the use of large components of pure zirconia at high temperatures results in spontaneous failure. The transformation from the tetragonal phase to cubic is also reversible and takes place at 2370 °C. Pure zirconia can be used only in the powder form, and therefore for uses that do not require consolidation into a massive part (e.g. as a starting product for the manufacture of ceramic enamels), as it breaks up during cooling due to the martensitic $t \rightarrow m$ transition [37].

The most striking characteristic of zirconia is that it exhibits phase transitions that were regarded for a long time as drawbacks but which, since 1975, have proved to be a rich source of possibilities [37, 110, 111]. Volume changes have been used to improve both the toughness and strength of zirconia-based ceramics. The addition of cubic stabilizing oxides, such as magnesia, calcia, yttria, or ceria, prevents from $t \rightarrow m$ transition over a wide temperature range (from room temperature to the melting point), as shown in Figure 1.9 [37, 111]. Fully or partially stabilized zirconia can be used\vadjust{\vfill\eject} to make monocrystals for jewelry, very similar to diamonds, crucibles and other refractory parts, thermal barriers, ionic conductors, and prosthetic biomaterials [37].

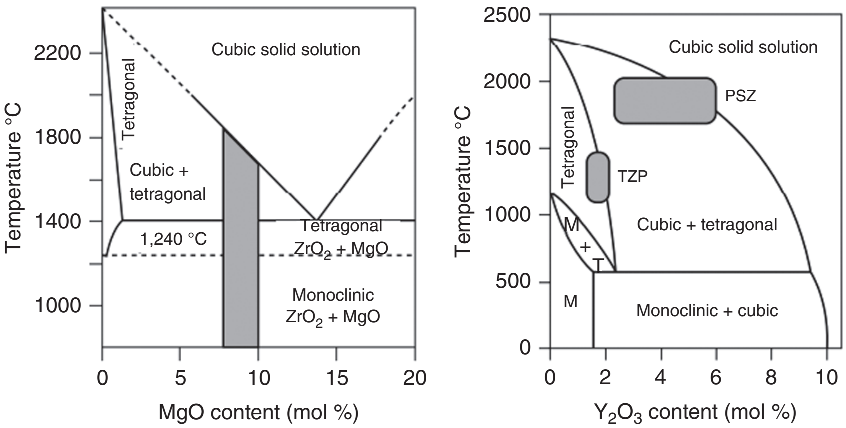

Figure 1.9 Phase diagrams of magnesia (MgO) and yttria (Y_2O_3)-stabilized zirconia. Source: Hannink et al. [112]/with permission of John Wiley & Sons.

The properties of zirconia are highly dependent on the crystal phases present, their concentration, size, and distribution. High-purity grade zirconia is obtained by the reaction of zirconium alkoxides, which in addition allows close control of particle size and size distribution. Hydrolysis of alkoxides is very rapid and leads to precipitation rather than gel formation. The precipitate, with a particle size of only a few nanometers, forms agglomerates that, if sufficiently large, settle out of solution. Under suitable conditions, however, the agglomeration process leads to the formation of a stable zirconia sol. Two types of agglomerates – spherical or open agglomerates – are obtained depending on the alkoxide starting material. Continuous coatings can be made from the open agglomerates by the dipping technique. Another method involves the conversion of a fluid colloidal suspension (sol) to a semirigid colloidal dispersion (gel) [111].

Zirconia is an inert material and features high corrosion resistance and a lack of etchability. Zirconia's chemical properties depend on preparation methods. Calcined zirconia is insoluble in all acids except hydrofluoric acid [40]. In strongly acidic solutions, the solubility is controlled by the formation of polynuclear hydrolysis species; in strongly alkaline solutions the solubility increases with increasing pH due to the formation of the zirconate ion ZrO_3^{2-} but not $Zr(OH)_5^-$. A solubility minimum occurs between pH 2 and 13 indicating that the dominant species in equilibrium with zirconium dioxide and hydrous zirconium oxide is the neutral species $Zr(OH)_4^0$ [113].

Yttria-stabilized zirconia (YSZ) is stable in oxidizing atmospheres at temperatures even as high as 1200 K. It is an excellent oxygen ion conductor and widely used as an electrolyte in solid oxide sensors and fuel cells [66].

1.3.3.2 Applications of Zirconia: Some Examples

Like titania, zirconia has been considered an alternative material to silica for liquid chromatography. In comparison to silica, zirconia stationary phases offer higher stability outside the pH range of 2 and 8 [114] and higher thermal stability at temperatures higher than 100 °C [115, 116]. Some examples of various zirconia stationary phases employed for proteins, nucleotides, organic acids, amines, basic drugs, and so on are reviewed in [117].

The possibility to operate at high temperatures can reduce the quantity of organic solvents needed, increase analyte mass transfer rates, decrease column back pressure, and reduce total analysis time significantly [116]. Using zirconia- and titania-based packing, a fast separation of alkylbenzene derivatives is possible, and such a system can operate at a temperature of 200 °C and pressures up to 10 000 psi, thus reducing eluent viscosity and enhancing mass transport. This permits to operation at very high linear velocities without sacrificing separation efficiency [115].

Due to its biocompatibility, high drug-loading capacity, easy surface conjugation of biomolecules, and excellent stability, the application of inorganic nanomaterials like zirconia in drug delivery has, therefore, attracted increasing research attention. Hollow mesoporous zirconia nanocapsules exhibit a high loading capacity of chemotherapy drugs like doxorubicin. The doxorubicin-loaded capsules have a pH-dependent release behavior, and the lower the pH, the faster the drug-releasing rate [99]. Porous, fluorescent zirconia particles have been investigated for drug-delivery applications. Such particles (∼380 nm in diameter) were prepared by the sol–gel method without template molecules or labeling dyes. The porous structure was the result of aggregation-induced particle formation. The inherent fluorescence of the particles was assigned to coordinatively unsaturated Zr^{4+} ions at the sol–gel-derived ZrO_2 surface. Doxorubicin complexes coordinatively unsaturated Zr^{4+} ions without dislocation, while carboxyl-bearing drugs interacted with basic surface Zr–OH sites, eliminating some of the carbonate species. The adsorption of ursolic acid at the zirconia surface shifted the IEP of the surface considerably, providing kinetic stability to the particles at physiological pH [118].

Yttria-stabilized zirconia is one of the most widely used oxygen ion conductors with applications in solid oxide fuel cells, oxygen pumps, and chemical sensors. In all of these applications, YSZ acts as a solid electrolyte where oxygen ions diffuse through the YSZ matrix as long as the operation temperature is above that required for oxygen ion transport ($T > 300$ °C) [66]. The discovery of the oxygen ion-conducting solid electrolyte and the ability of an electrochemical cell based thereon to measure oxygen potential led to a breakthrough in continuous oxygen concentration measurement. Many industrial processes are based on reactions that directly involve oxygen, and it is often important to measure, monitor, and control oxygen concentration to ensure product quality, optimize fuel consumption, and minimize pollution. This applies to processes that include the extraction, refining, and production of iron, steel, and other metals and alloys; the manufacture of glass and ceramics; heat treatment; fluidized bed combustion; and indeed, most high-temperature industrial environments; kilns, furnaces, and boilers [111]. The zirconia oxygen sensor was first demonstrated in 1965, and thereafter, intensive development has resulted in its widespread use.

Glass electrodes are commonly used for pH measurements, but their operation is limited by temperature and inaccuracy in basic solutions. Yttria-stabilized zirconia showed excellent response to pH when incorporated into structures similar to the conventional glass electrode while being usable in critical monitoring sites, for example, in high-temperature solutions such as geothermal brines, water in nuclear power reactors and power plants, chemical processing plants, and other installations [111].

Zirconia high-temperature hygrometers utilize the principle that oxygen concentrated in air is diluted by water vapor, and the amount of water vapor can be obtained by measuring the concentration of oxygen using a zirconia sensor. The hygrometer can be used at up to 600 °C in applications such as the control of airflow in air conditioning units and drying apparatus, for the control of heater units and the recycling of hot gases. The advantages of zirconia-based humidity sensors are their high sensing capability, precision and reliability with little change in characteristics with time, quick response, and their sensitivity is little affected by frequency and voltage [111].

1.3.4 Silica

Silicon oxide, or silica (SiO_2), is by far the major component of the earth's crust and perhaps the most important and versatile oxide compound. It is widely available as a raw material on the earth's surface, but crystalline and noncrystalline silicas can be synthetically obtained [119]. Silica is a fundamental constituent of a wide range of ceramic products and glasses, and it has widespread industrial applications as a basic compound both for ceramists and glassmakers, as food additives (anticaking agent, viscosity controller, antifoaming agent, dough modifier, excipient in drugs and vitamins) [120], as drug-delivery devices, and bone-repairing systems [121]. Functionalized submicrometer-sized silica spheres are applied in chromatography [44, 45], selective separations, and biological immunoassays [122]. Silica microbeads can be incorporated into microfluidic devices, thus enhancing their sensitivity for detection of trace amounts of biological molecules [123].

1.3.4.1 Properties of Silica

Silica exists in a wide variety of crystalline and noncrystalline forms under different conditions of temperature and pressure, which are possible because of the flexibility of the linkage among SiO_4 tetrahedra. The phase diagram of silica is shown in Figure 1.10, and the crystal structures in Table 1.3.

Quartz is the thermodynamically stable, room temperature polymorph, and it forms low (α) quartz and high (β) quartz. Quartz is itself a widely available mineral and is an ingredient in many commercial ceramics and glasses. Cristobalite is the crystalline silica polymorph at atmospheric pressure above 1470 °C. It has a *fcc* lattice with 24 ions per unit cell, and it is the simplest form of silica. There are other thermodynamic stable polymorphs (e.g. coesite, stishovite, tridymite). Coesite and stishovite are both stable at high pressures. At room temperature, coesite is stable at pressures above ∼2 GPa, and stishovite is stable at pressures above ∼7.7 GPa. Other metastable SiO_2 synthetic polymorphs exist and these include vitreous silica, clathrasils, and zeolites. Except for stishovite, all these structures are based on frameworks of SiO_4 tetrahedra. There are several water-soluble forms of silica referred collectively to as silicic acid (ortho-, meta-, di, and tri-silicates), which are present in surface and well water in the range of 1–100 mg/l [119].

Under ambient conditions, α-quartz is the thermodynamically favored polymorph of silica, and it is transformed into β-quartz at 573 °C, which has a similar structure but with less distortion. During this transformation, the optical activity of quartz is preserved. When heated to 867 °C, β-quartz transforms into β-tridymite. This transformation involves the breaking of Si—O bonds to allow the oxygen tetrahedra to rearrange themselves into

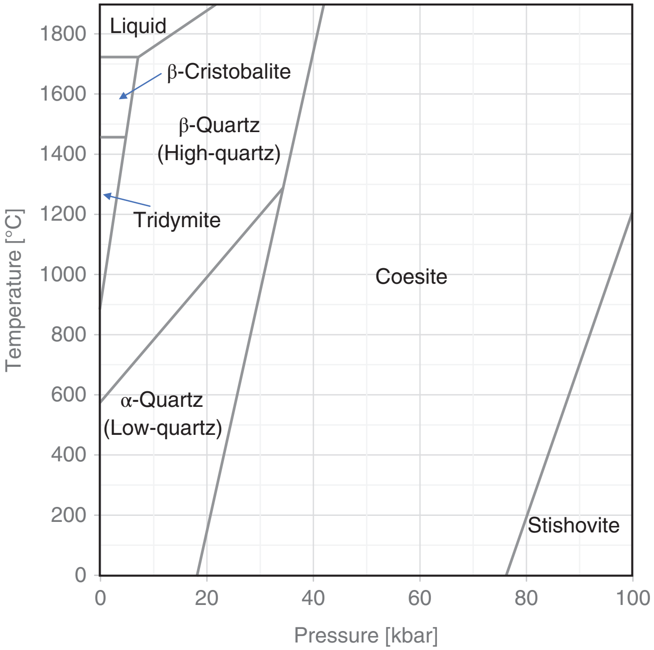

Figure 1.10 Phase diagram for the silica system. Source: Adapted from Lakshtanov et al. [124].

Table 1.3 Crystal structure and physicochemical properties of silicas.

Designation	Structure	Lattice parameters (Angstrom/angle) *a*	*B*	*C*	Density (g/cm^3)
Low-quartz (α)	Trigonal	4.91304		5.40463	2.65
High-quartz (β)	Hexagonal	4.91304		5.40463	2.53
α-Cristobalite	Tetragonal	7.16/90	7.16/90	7.16/90	2.33
β-Cristobalite	Cubic				2.27
Coesite	Monoclinic	7.143	12.383	7.143	3.01
Stishovite	Tetragonal	4.1772		2.6651	4.29

Adapted from Shackelford and Doremus [119].

a simpler, more open hexagonal structure of lower density, and the quartz–tridymite loses some of the optical activity. Beta-tridymite heated at even higher temperatures to 1470 C gives β-cristobalite, which resembles the structure of diamond. Melting of cristobalite takes place at 1723 °C. Vitreous silica, which is obtained by slow cooling of silica melt, has less long-range order but retains the short-range order of the silica tetrahedron and features a high degree of randomness [119]. A schematic of silica transformation at different temperatures is shown in Figure 1.11.

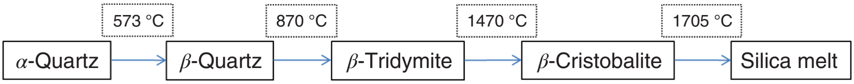

Figure 1.11 Silica transformation at different temperatures.

Typically, silica is insoluble in all acids except for hydrogen fluoride, and it dissolves in bases like KOH and NaOH solutions. However, discordant data are found in the literature because of the differences and properties of the analyzed materials [125–128].

Whenever silica comes in contact with water, the dissolution involves a chemical reaction or hydrolysis in an excess of water, and it involves hydration and dehydration reactions catalyzed by OH-ions:

$$SiO_2 + 2H_2O \rightarrow Si(OH)_4$$

Although silica is abundantly present in natural sources, different techniques for synthetic production have pushed its application range. Large, high-quality crystals of quartz can be grown by well-established methods like hydrothermal growth in autoclaves, vapor phase hydrolysis, and the sol–gel method [119]. Among these methods, sol–gel has been extensively investigated for the synthesis of silica materials with different morphologies and sizes, both as glassy or as crystalline solids, and for use in several impressive applications. Thanks to its high versatility, the sol–gel process has permitted the creation of materials and hybrid systems for efficient drug and gene delivery, catalysts, chromatography, biochemical reactors containing biological species such as enzymes, whole cells and even bacteria, sensors, surface coatings, imaging systems, tailored organic light-emitting diodes (OLEDs), and so on [129].

A very important class of silica materials is mesoporous silica, which has become apparent as a promising and novel drug vehicle for target drug delivery. Mesoporous silica materials were discovered in 1992 by the Mobile Oil Corporation and have since gotten a lot of attention because of their superior textural properties like high surface area, large pore volume, tunable pore diameter, narrow pore size distribution, and external and internal surfaces that can be selectively functionalized with multiple organic and inorganic groups and biological entities [130–132]. Nanoparticles of mesoporous silica have received particular attention as a promising and novel drug vehicle. Thanks to the porous structure and large surface area of the solid framework, chemical stability, and biocompatibility, it is possible to attach different functional groups for targeting the drug moiety and the surface functionality and ensure a controlled release and target drug delivery of a variety of drug molecules.

Mesoporous silica can have different arrangements, and some structures are exemplary, as shown in Figure 1.12. SBA-15 (Santa Barbara Amorphous) is a mesoporous silica with cylindrical pores arranged in a hexagonal structure. For this material, the pore size refers to the width of the cylindrical pores, which can be tuned between 5 and 26 nm, even though pore sizes above 12 nm are rare. The length of the pores can vary from ~200 nm to several microns. A microporous network, called the corona, surrounds each mesopore, and this interconnects the mesopores with each other and is responsible for the high surface area, which is about 500–1000 m^2/g [132, 133].

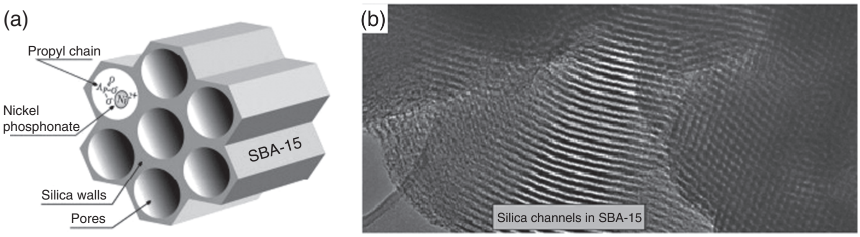

Figure 1.12 (a) Schematic of the structure of functionalized mesoporous silica SBA-15. (b) TEM of silica channel in SBA-15. Source: (a) Laskowski et al. [132]/with permission of Elsevier. (b) Gibson [133]/Reproduced with permission of Royal Society of Chemistry.

1.3.4.2 Application of Silica: Some Examples

Silica-based materials find uncountable applications in many sectors. Silica is heavily used for purification and synthesis purposes based on liquid chromatography [44, 134, 135]. This technique is fundamental for several analytical purposes for the pharmaceutical, biotechnological, biomedical industries and environmental studies. Other typical applications are food safety testing, studies and high-throughput analysis of amino acids, peptides, drugs and metabolites, and other bioanalytes, as well as bioanalytical separation. Functionalized silica offers several advantages over traditional functionalized polymers as it is thermally and mechanically stable and it does not suffer from swelling or shrinking in any solvent. Due to surface functionalization, the rate of reaction is faster as it is not controlled by diffusional processes into and out of the polymer and loading is more controllable. For liquid chromatography, high-purity, metal-free, monodisperse silica spheres with well-defined particle size, high surface area, and tailorable pore size are required. In addition, the surface of such particles is modified and decorated with octyl, octadecyl, phenyl, and other functional groups that can improve selectivity, resolution, and separation in the column. Silica scavengers, specifically functionalized silicas designed to react and bind excess reagents and by-products, permits the simplification of the purification processes. These rely on chemically driven reactions where the excess reagents and reaction by-products react with and bind to the scavenger [129].

Another main application area of silica-based materials in biotechnology is drug delivery and biosensing, or a combination thereof. At the very beginning, silica nanoparticles were used for controlled delivery of various hydrophilic or hydrophobic active agents Functionalization of the inner pore system and/or of the external surface, and encapsulation rendered them as promising drug-delivery vehicles for the treatment of different types of diseases, like cancer, bacterial infections, inflammation, and so on [136–142], but also for consumer products, like cosmetics [142]. An outstanding example is sunscreen cosmetic products as inert glassy silica microparticles can encase high concentrations of sunscreen molecules within a thin shell of inert sol–gel glass [129]. Functionalization and encapsulation in silica matrixes are still hot topics both in fundamental research and in industry because of the possibility to eliminate processing steps, use less of an expensive ingredient, or incorporate a new ingredient that would not work without encapsulation. E.g. through the sol–gel microencapsulation, higher drug or active agent loading can be achieved (even more than 80% of the weight of the particles), and thus a sustained delivery of the active ingredients under defined mechanical or chemical conditions can be achieved.

Many challenges of oral systemic therapy or intravenous drug administration, such as limited biodistribution and the need for higher doses; poor gastrointestinal drug solubility or poor selectivity; rapid drug metabolization and excretion; and side effects due to systemic exposure, have been overcome by silica-based drug-delivery vehicles [136, 143]. To tackle these aspects, an effort has been made to create small devices that can be easily loaded with drugs, delivered with minimal trauma, easily tracked, programmed, and controlled by specific stimuli, and, last but not least, inexpensively manufactured [129, 144].

Functionalization and coating of silica with organic molecules have been used to improve biocompatibility, facilitate the attachment of targeting ligands for specific recognition, and enhance drug encapsulation. The functionalization with different probes, such as fluorescent markers, organic or inorganic dyes, or particles, can help to track the materials within living cells or organisms and evaluate target specificity and delivery [136, 145–149]. A schematic of a functionalized silica carrier with potential use for the above-mentioned applications is given in Figure 1.13.

It must be kept in mind that the silica matrix can also be designed in order to ensure a better and more tightly controlled release of the active substance and provide a better therapeutic effect in situ. A number of silica-based ceramic particles with independent control over the release rate and particle size have been synthesized by combining sol–gel technology with water-in-oil (W/O) emulsions [136, 149–151] (Figure 1.14). The typical particle size can be varied from a few nanometers to 100 μm, and it can be controlled by the emulsion chemistry. Sol–gel emulsions are more effective because they enable the production of either micro- or nanoparticles with homogeneous distribution activity and permit ambient temperature processing, which is necessary for handling temperature-sensitive biological agents [129].

Silica has been widely used as a solid support for biocatalytic systems, which can offer several advantages over conventional synthetic catalysts, as they do not demand harsh chemical conditions, permit an easy recovery of both product and enzyme, and represent a more sustainable approach for the production of chemicals, pharmaceutics, fuels, and energy [152]. Moreover, immobilization of enzymes is generally used to improve protein stability as the porous structure provides a protective environment where the enzyme can

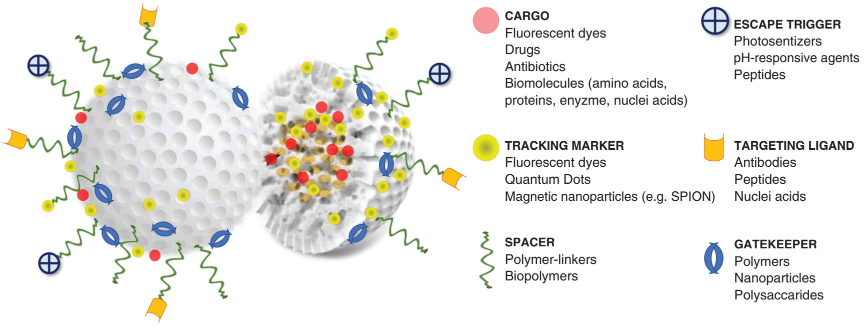

Figure 1.13 A scheme of functionalized nanosized mesoporous silica particles for drug delivery and monitoring. Source: Adapted from Argyo et al. [144].

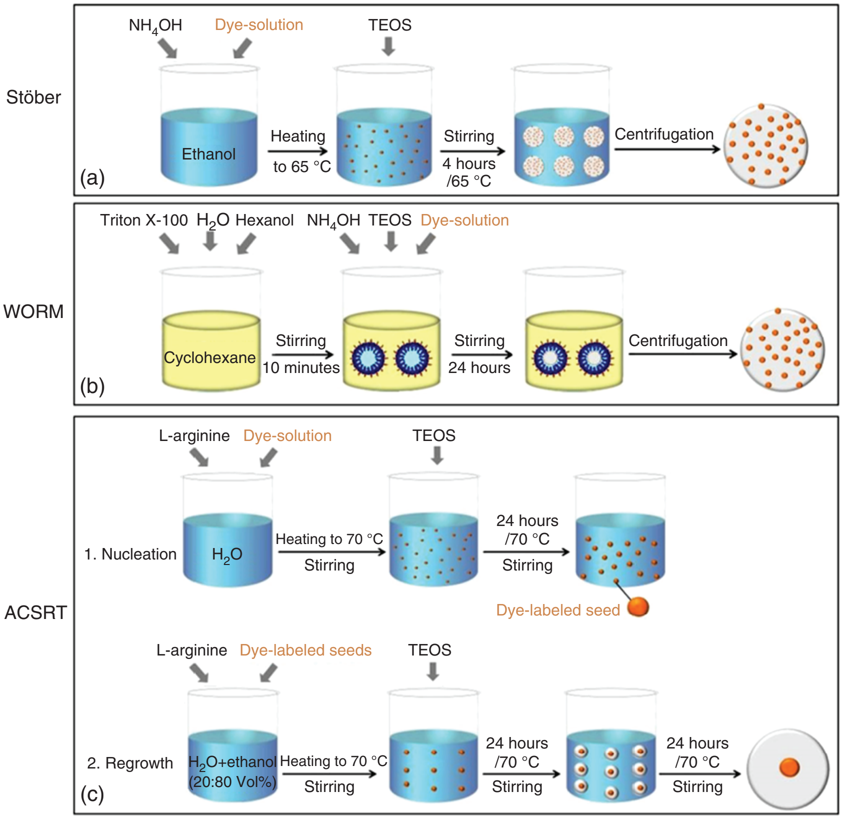

Figure 1.14 Schematic illustration for synthesis of fluorescent silica NPs with three different methods including Stoeber (a), water-in-oil reverse microemulsion (WORM) (b), amino acid-catalyzed seed regrowth technique (ACSRT) (c). Source: Shahabi et al. [150]/with permission of Springer Nature.

tolerate extreme pH values or pH variations, higher salt concentrations, and temperatures [152–154].

Protein immobilization or encapsulation is a rather widespread approach, but there are still several issues to be solved [152]. Typically, little is known about how the enzyme is affected during and after immobilization. This is routinely monitored by comparing the enzymatic activity of the immobilized enzyme with that of the free enzyme. However, this must be taken with reservation because factors such as enzyme inactivation during immobilization, enzyme orientation, changes in the enzyme structure, and the different microenvironment inside the pores compared to the bulk solution can influence the activity of the enzyme. The individual contribution and the extent of the influence on the enzymatic performance are often poorly definable, thus making it difficult to elucidate the causes of any changes in the specific activity. These uncertainties cause several challenges in the rational design of biocatalysts and in predicting their performance [153].

Silica-based materials are not limited to medicine and biology but find large applications for other demanding and challenging issues. Mesoporous silica is one of the most versatile and efficient adsorbents for removing inorganic and organic environmental pollutants. The possibility to manipulate and tailor the structural, morphological, and surface properties is known to greatly improve the adsorption capacity and selectivity for a wide range of different pollutant types [155–158]. For environmental monitoring and, in general, in all contexts requiring rapid and accurate measurement of one or more analytes, silica can be employed for chemical sensing. Silica is ideal for sensing purposes because of its chemical inertness, low or nontoxicity, and optical transparency. Chemical changes in the environment of the entrapped molecule are sensed and revealed, for example, through color-developing reactions between an entrapped reagent and an external diffusible chemical species or through the emission of light. Reactions include traditional chemical proton transfer reactions (such as pH indicators), redox reactions, complexations, and ligand exchanges as well as biochemical enzymatic reactions to reveal analytes such as H^+, metal ions, inorganic anions, glucose, oxygen, and ammonia [159–162].

1.3.5 Iron oxide

Another important oxide is iron oxide, which has a plethora of applications not only in biotechnology but also in the environmental field. For example, ferrites are widely used in conventional electronic, electrical, and magnetic devices. For the past two decades, since the discovery of the superparamagnetic nature of nanostructured ferrites, their applications in biotechnology, biomedical sciences, and microbiology have gained immense attention [163, 164]. Iron oxide nanoparticles (IONs) have been used as nanosources of heat for hyperthermia in tumors or in infected tissues [164]. Like silica particles, magnetic nanoparticles can be functionalized with multiple and different polymers and biomolecules, which can impart higher biocompatibility and facilitate their *in vivo* uptake. A schematic of a multi-functionalized magnetic particle and a striking example of anticancer therapy are shown in Figure 1.15.

Antibiotic-loaded IONs are used for targeted delivery of chemical therapy direct to the infected organ, and IONs have been used as a dirigible carrier for more potent antimicrobial nanomaterials, for specific separation of pathogenic and nonpathogenic bacterial strains, or for magnetic immobilization of microbial cells and process intensification in a biotechnological process [165].

Research and publications on iron materials (especially nanoparticles) have *boomed* in recent years. We intend here to mention some selected references on the topic. For a deeper reading on synthesis and surface engineering and applications, we recommend, for example, the following references [164, 166–168].

1.3.6 Barium Titanate

Barium titanate ($BaTiO_3$) is known as the oldest ceramic belonging to the perovskite family, and it can be a dielectric or a semiconductor, depending on its doping and its stoichiometry. Its ferroelectric and dielectric properties have been known since the early 1940s [169]. $BaTiO_3$ is traditionally used for electrical and electronic devices; it is not only one of the

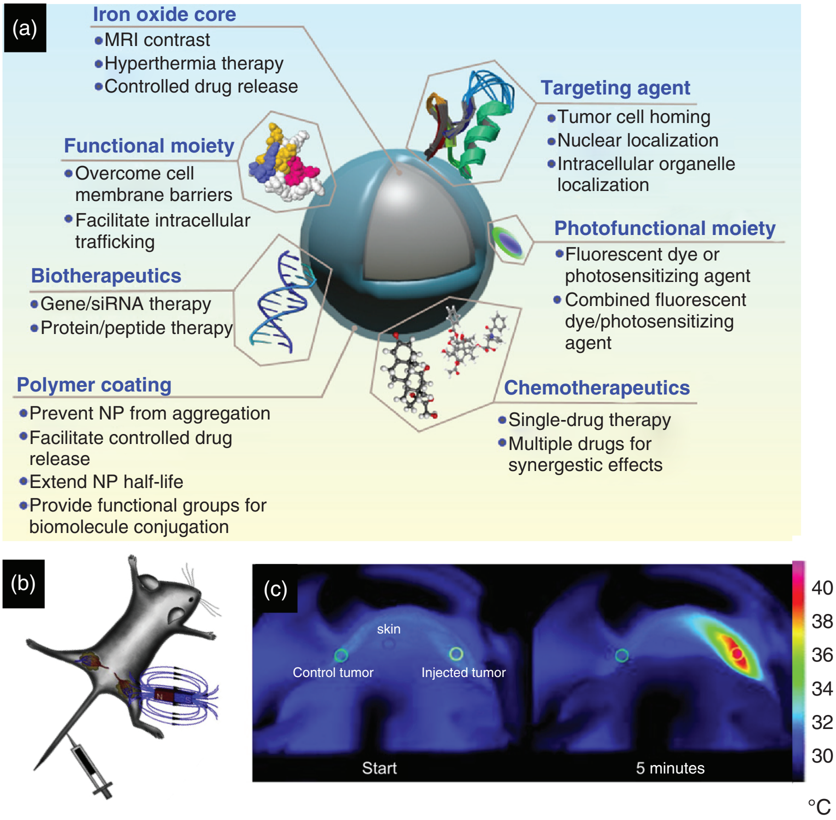

Figure 1.15 (a) Schematic illustration of a fully functionalized iron oxide nanoparticle for theranostics. The peculiarity of such particles is their multifunctionality: the magnetite core serves as an MRI contrast agent and heat source for magnetic hyperthermia, the polymeric coating increases biocompatibility, mitigates the reticuloendothelial system (RES) uptake, and allows for facile decoration with drugs (chemotherapeutic and/or biotherapeutic), optical enhancement, and targeting moieties. (b) A schematic drawing to illustrate in vivo magnetic tumor targeting. (c) Magnetite NP-induced magnetic hyperthermia and its effect on the growth of solid tumors in mice. Thermographic infrared photographs show the heat development during exposure to an alternating magnetic field of a mouse intratumorally injected with iron oxide NPs. The scale bar on the right indicates the color code of the surface temperature. Source: (a–c) Adapted from Revia and Zhang [164]/with permission of Elsevier.

basic materials for ceramic capacitors but also used for the manufacture of various types of probes and sensors, and it is a well-known substitute for common lead-based systems [169]. In the last decade, $BaTiO_3$ has attracted attention for biomedicine or, more generally, for biotechnological applications. An increasing number of studies have been focused on the exploitation of $BaTiO_3$ nanoparticles in the biomedical field, owing to their high biocompatibility and their peculiar nonlinear optical properties that have encouraged their use as nanocarriers for drug delivery, label-free imaging probes, and nanotransducers for cell stimulation [170, 171]. Recently, $BaTiO_3$ has been used to fabricate piezoelectric bioceramics

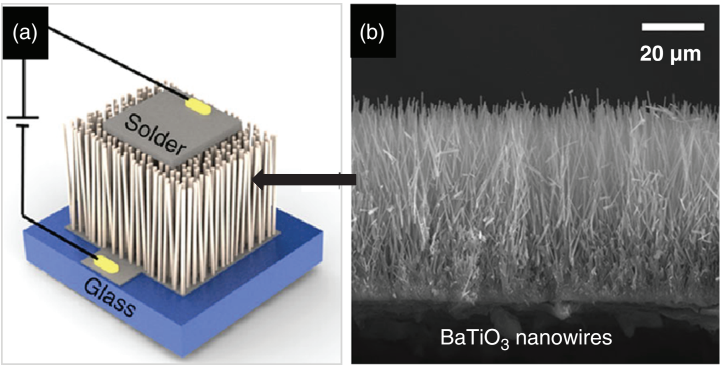

Figure 1.16 (a) Schematic diagram of sensor device using vertically aligned piezoelectric $BaTiO_3$ nanowires. (b) A cross-sectional SEM image of $BaTiO_3$ NW arrays. Source: Adapted from Koka and Sodano [175]/with permission of Springer Nature.

for bone regeneration, exploiting the beneficial effect of piezoelectricity on bone growth promotion [172, 173].

$BaTiO_3$ also finds application in biotechnology as a piezoelectric material for enzymatic biosensors and immunosensors [45] and for energy harvesting [174, 175]. A $BaTiO_3$ sensor consisting of a vertically aligned piezoelectric nanowire array as an accelerometer is shown in Figure 1.16.

1.4 Nonoxide Ceramics

Advanced nonoxide ceramics are typically divided into four categories according to their bonding types and the properties resulting therefrom, such as high melting points, hardness, strength, and stiffness. Nonoxide ceramics are:

(a) hard elements such as carbon (diamond) and boron;
(b) hard ceramics formed as compounds of transition metals of groups IVa (Ti, Zr, Hf), Va (V, Nb, Ta), and VIa (Cr, Mo, W) of the PSE with B, C, N, and Si;
(c) binary and ternary compounds containing elements from groups IIIb to Vb (B, C, N, and Si);
(d) some salts like halogenides and chalcogenides, such as refractory fluorides (CaF) and sulfides (BaS, CeS).

Until 1970, nonoxide ceramics were primarily used in the iron and steel industries or in the chemical industry [37]. Afterwards, the need for the new high-performance ceramics for various technically and economically relevant sectors (mechanical engineering, aeronautics, electronics, nuclear power) has strongly pushed their development in other sectors like biotechnology and biomedicine.

Unlike oxide materials, the raw materials necessary for the production of these nonoxide ceramics are not found in nature but are made synthetically [176]. In the following, a brief overview of some relevant nonoxide ceramics, which find usage for medical, biotechnological, and environmental purposes, is given.

1.4.1 Nitrides

Nitrides primarily include silicon nitride and compounds based on nitride-oxide or oxynitride systems (e.g. β′-sialons), aluminum nitride (AlN), and various metallic nitrides, for example, *titanium nitride* (TiN). The favorable combination of properties that nitrides possess – high strength over a broad temperature range, high hardness, moderate thermal conductivity, low coefficient of thermal expansion, moderately high elastic modulus, and unusually high fracture toughness for a ceramic – leads to excellent thermal shock resistance, the capacity to withstand heavy structural loads at high temperatures, and superior wear resistance [29].

Here, only silicon nitride (Si_3N_4) will be considered. Silicon nitride can be produced via the reaction of silicon with nitrogen to form Si_3N_4 by carbothermal reduction (reaction of quartz powder with ammonia) or from the gas phase with silicon tetrachloride [176]. It has excellent thermal shock resistance and high-temperature strength; lower elastic modulus than alumina; a significantly smaller coefficient of thermal expansion; and on oxidation, it forms soft, often protective, silica films. These properties make it ideal for use in automotive engines and gas turbines, for example, for turbocharger rotors, glow plugs, and hot plugs in diesel engines. Si_3N_4 is being applied in many other diverse biotechnological applications, for example, as thin windows for biomedical microdevices [177], MEMS [21], windows for electron microscopy of whole cells [178], and sensors for interference-based detection of nucleic acid targets [179]. Due to its biocompatibility, stability *in vivo*, and superior mechanical properties, Si_3N_4 is considered an attractive ceramic implant material for orthopedic surgery, for example, in spinal fusion surgery, as bearings in joint replacement, and it is being considered for dental implants. Si_3N_4 implants are currently created using conventional ceramic-processing techniques, but new manufacturing processes like additive manufacturing could be used to create customized implants with precise anatomical shape, dimension, and well-controlled microstructure. Moreover, its surface chemistry can be varied from a silica-rich to a predominantly silicon-amine composition, which can influence the *in vivo* response of cells, bacteria, and tissues. Si_3N_4 implants have shown attractive osseointegration and antimicrobial activity *in vivo*, while Si_3N_4 bearings have shown low wear rates when articulating against themselves or against polyethylene [180–183].

1.4.2 Carbides

Carbides can be considered the main category of nonoxides and, among them, the most important are silicon carbide, boron carbide, and tungsten carbides.

Silicon carbide (SiC) is a covalent compound that can exist in the cubic or hexagonal crystal structures. To be thorough, it should be noted that SiC occurs naturally in the form of moissanite, a natural mineral, in the Canyon Diablo meteorite crater in Arizona, as well as the Murchinson carbonaceous chondrite [1].

Silicon carbide (“carborundum”) is known as one of the most important structural ceramics and because of its properties, such as strength retention at high temperatures, oxidation resistance, wear resistance, and thermal shock resistance, it has long been used exclusively as a hard and durable material in abrasive metal-machining operations such as grinding, sandblasting, and water-jet cutting. Because of its positive temperature coefficient of electrical conductivity at elevated temperatures, SiC is used for heating elements in high-temperature furnaces for melting and casting metals as well as for heat exchanger tubes in the chemical process industry.

Today, because of its resistance to high temperatures, aggressive chemicals, and abrasion and its semiconducting properties, SiC is used for many other applications in harsh environmental conditions. Because of these properties, together with low weight, no toxicity, and biocompatibility, SiC has been reconsidered as a very promising material for implantable parts and biotechnological purposes [184]. Porous SiC is applied for bone implants [185, 186], as filtering media for critical applications like microdialysis or protein separation by molecular weight, for bio-microelectromechanical systems (bioMEMs) [187], for detection and diagnosis of diseases in the area of photoluminescent dye markers [188–190].

Boron carbide (B_4C) is another of the hardest materials known, following cubic boron nitride and diamond. It is characterized by a unique combination of properties that make it the material of choice for a wide range of engineering applications. Synthetic B_4C is used in abrasive and wear-resistant products, in hard lightweight composite materials, for high-temperature thermoelectric conversion, and in the nuclear industry as a protective barrier and neutron speed reducer. Nowadays, B_4C nanoparticles, nanodots, or nanopowders are spherical high-surface area particles considered for application in biomedical and bioscience areas, and more specifically as a promising boron agent for boron neutron capture therapy (BNCT) [191–193].

Another relevant carbide is tungsten carbide (WC), which exhibits high electronic conductivity because of its metallic band structure. WC is designed for wear-resistant surfacing of parts operating under conditions of intense wear. It is used for the surfacing of drill bits, blast furnaces, mining tools, orthopedic surgical instruments, and dental burs.

1.5 Carbon-based Materials

Carbon has a unique structure–property relationship. Carbon has various allotropes with very different properties, and it forms stable substances with reaction partners with different electronegativity. Carbon-based materials have a broad range of applications in medicine because of their structural versatility [194], and some examples will be given in detail in Chapter 9. The different allotropes permit different functionalization and surface modification that enable a specific tailoring of different properties. Carbon is used in different forms: diamond, graphite-based materials, fibers, and compounds, nanotubes, graphene, and amorphous carbon. Pyrolytic carbon is a synthetic form of carbon with a structure similar to graphite. It was proposed as a coating for orthopedic implants because of its similar elastic modulus to cortical bone and its thromboresistant character. Nevertheless, heart valve devices have gained a significant market in the biomedical area [192]. Carbon-based absorbents are furthermore considered to be the best candidates for water filtration, water/oil separation, oil-spill clean-up, wastewater treatment, gas separation, and purification, as they possess high surface area, low density, excellent mechanical properties, good chemical stability, environmental friendliness, and large pore volume. For such purposes, different types of carbon-based materials can be used, such as carbon aerogels, graphene or carbon nanotubes, coated sponges, carbon nanotube forests, graphene foams or sponges, carbon coatings, activated carbon, porous carbon nanoparticles, and carbon fibers [195].

Carbon fibers, also called graphite fibers or carbon graphite, may be used by themselves or can be reinforced with other materials. Because of their light weight, flexibility, high strength, and high tensile modulus, several commercial products incorporating carbon fibers have been developed as implant reinforcement fillers and replacements for ligaments and tendons [194, 196].

Fullerenes, an allotrope of carbon with 60 carbon atoms arranged in a spherical structure, have been the subject of intense research, both for their unique chemistry and for their technological applications, especially in bio- and nanotechnology [197–199]. Several functionalization strategies using cyclodextrins, phospholipids, liposomes, and polyvinylpyrrolidone, among others, have been developed to overcome their lack of solubility in polar solvents and thus make fullerenes applicable for delivery into aqueous media [200, 201]. Nowadays, many fullerene-based compounds have been synthesized and presented as potentially useful in anticancer or antimicrobial therapies; enzyme inhibition; controlled drug delivery; diagnostic imaging; and antiviral activators. As fullerenes absorb in the UV and visible regions of the spectrum, they are used for inducing photodynamic damage to biological systems and as photo-induced enzyme inhibition agents and to convert reactive oxygen species (ROS) involved in cellular signaling and damage [192].

Carbon nanotubes (CNT) are long, hollow structures with walls formed by one atom-thick sheets of carbon and have the highest strength of any material known, the highest thermal conductivity, and outstanding field emission properties [192]. Because of the chemical inertness of the graphitic walls, functionalization with covalent or noncovalent bonding is often required. Functionalized CNT has different applications. Among others, they are employed as scaffolds for tissue engineering and nerve cell growth [202–204], as a reinforcement material for bioactive ceramics, electrically stimulating composites to accelerate the osteointegration process, gene transfection vectors or as hyperthermia agents [205], for cancer treatments [206] and drug delivery [192, 207, 208].

Graphene represents one of the most promising “nanomaterials” of the last few years. Owing to its unique physicochemical properties such as good sensing ability and excellent mechanical, thermal, and electrical properties, graphene has been the focus of basic research and technological applications [209]. However, robust methods for producing chemically functionalized graphene in large quantities are still lacking [210]. Graphene and its derived structures (graphene oxide, graphene platelets, graphene nano flakes) have become popular materials for fabricating electrode matrices/supports for sensing and biosensing, for example, for biomolecule immobilization to improve electrochemical detection [209]. Graphene finds applications as a nanocarrier for loading anticancer drugs, as a biosensor for sensitive and selective detection of proteins, for example, for the detection of cancer biomarkers [211], glucose sensors [212], enzyme-graphene nanocomposites for H_2O_2 and cholesterol detection [213, 214], and biosensor for ethanol [215]. Graphene-based analytical techniques can also be applied for monitoring chemical species of environmental relevance and contaminants such as heavy metals, pesticides, phenol compounds, among others [209, 216, 217]. Filters made of graphene can remove airborne biological contaminants. Graphene foams are being explored for selective gas–water–oil separation, spilled oil collection, and water cleaning [195, 218–221]. Self-sterilizing graphene filters grab airborne pathogens and kill them with small pulses of electricity. Such filters could also be used to catch other biological contaminants like fungi, spores, prions, and endotoxins carried by droplets, aerosols, and PM [222]. Three-dimensional graphene foams can selectively filtrate gas–water–oil filtration and have numerous potential practical applications to prevent possible environmental pollution and machine/facility malfunctions in oil-based industries [223].

Diamond is mostly used as a bioinert coating, acting as a barrier diffusion layer and/or autolubricant. Diamond also has high resistance to bacterial colonization when compared with medical steel or titanium. In addition to its use in total hip or knee replacement, it has been proposed as a coating for retinal microchips to restore retinal degeneration [224]. Studies on its hemocompatibility proved that it presents minimal plasma protein adhesion and no thrombogenic properties, so it has been used as a coating for heart valves, catheters, or stent coatings [192].

More details on the potentialities and applications of functionalized carbon-based materials can be found in a separate and dedicated chapter (*Chapter 9*).

1.6 Conclusions

This first chapter aims at illustrating the basic properties of ceramic materials and exemplarily presents some applications for biotechnological, medical, and environmental purposes, as well as some potentialities and future perspectives.

A forecast of the type of ceramic and application fields of highest interest for the next decade is presented in Figure 1.17.

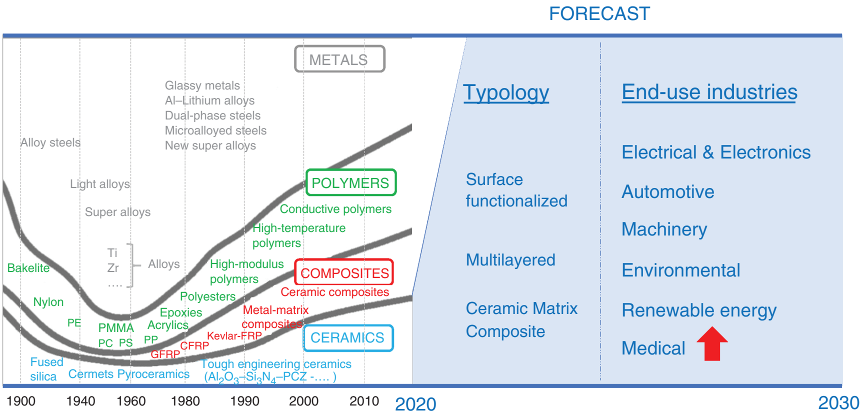

Figure 1.17 Forecast of ceramics by type and application field for the next decade. The red arrow indicates the expected rise in medical applications, which include diagnostic tools and new drugs, also as a result of developing countermeasures to the recent corona virus pandemic.

The bigger drivers are assumed to be the rising demand for renewable energy; clean technology and environmental safety; medical devices and diagnostic tools; and components for the electronics industry.

Oxide ceramics, thanks to their specific characteristics (e.g. biocompatibility, stability, and relatively "easy" surface modification), together with their suitability in a number of application areas far beyond those that could be highlighted in this book, account for the largest market share. Nonoxide ceramics have high acceptance in various end-use industries, such as electronics, semiconductors, and automotives. Their application for biotechnological, medical, and environmental purposes is far behind in comparison to oxides, but a larger usage and new systems are expected because of intensifying fundamental and applied research and development activities. Both oxide and nonoxide ceramics possess unique physical, chemical, electrical, optical, and mechanical properties that can be tuned and combined with surface modifications. This has led to new applications over the past several decades and will permit new opportunities in the future.

Similar considerations can be drawn for carbon-based materials, and there is an incredible volume of literature supporting their use and immense potential. However, there are several challenges and limitations to be overcome, for example, high production costs, uncertainties regarding ecological safety, and human health issues.

In conclusion, both ceramics and carbon-based materials are the basis for creating novel components designed to tackle the major challenges of the past and future decades, such as improving public health through improved drugs and diagnostics; bio-based chemicals; the climate crisis; environmental safety; and renewable energy production to reduce dependency on fossil fuels.

However, the scenario for the next few years could change in response to urgent needs like those occuring during the ongoing coronavirus outbreak. The pandemic has already hampered product demand in most industries and dictated a boom in the medical sector. Nevertheless, such a dramatic global challenge has shown the versatility and potential of ceramics more strongly than before. Ceramics are ideal carrier materials for diagnostic probes, in drug and vaccine production, and for purification, and the demand is expected to increase because of the race of pharmaceutical and med-tech companies to expand their testing capacities and propose new safe and efficient treatments in large volumes and available to the majority of the population.

References

1 Heimann, R.B. (2010). *Classic and Advanced Ceramics: From Fundamentals to Applications*. Wiley-VCH Verlag GmbH & Co. KGa.

2 Maggetti, R.B.H.M. (2014). *Ancient and Historical Ceramics*. Stuttgart, Germany: Schweizerbart Science Publishers http://www.schweizerbart.de//publications/detail/isbn/9783510652907/Heimann_Maggetti_Ancient_and_Historica.

3 Ashby, M.F., Bush, S.F., Swindells, N. et al. (1987). Technology of the 1990s: advanced materials and predictive design and discussion. *Philos. Trans. R. Soc. London Ser. A, Math Phys. Sci.* 322 (1567): 393–407. http://www.jstor.org/stable/37767.

4 Subbarao, E.C. (1991). A second ceramic age—a new materials frontier. *Bull Mater. Sci.* 14 (5): 1171–1182. https://doi.org/10.1007/BF02744610.

5 Somiya, S. (2003). *Handbook of Advanced Ceramics -Processing and Their Applications*, vol. 2 (ed. S. Somiya, F. Aldinger, F. Claussen, et al.). Elsevier Inc.

6 Li, C., Sun, W., Lu, Z. et al. (2020). Ceramic nanocomposite membranes and membrane fouling: a review. *Water Res.* 175: 115674. http://www.sciencedirect.com/science/article/pii/S0043135420302104.

7 Lahiere, R.J. and Goodboy, K.P. (1993). Ceramic membrane treatment of petrochemical wastewater. *Environ. Prog.* 12 (2): 86–96.

8 He, Z., Lyu, Z., Gu, Q. et al. (2019). Ceramic-based membranes for water and wastewater treatment. *Colloids Surf. A Physicochem. Eng. Asp.* 578: 123513.

9 Liu, L., Luo, X.-B., Ding, L., and Luo, S.-L. (2019). 4 - Application of nanotechnology in the removal of heavy metal from water. In: *Micro and Nano Technologies* (ed. X. Luo and D. F), 83–147. Elsevier.

10 Ramlow, H., Ferreira, R.K.M., Marangoni, C., and Machado, R.A.F. (2019). Ceramic membranes applied to membrane distillation: a comprehensive review. *Int. J. Appl. Ceram. Technol.* 16 (6): 2161–2172. https://doi.org/10.1111/ijac.13301.

11 Dommati, H., Ray, S.S., Wang, J.-C., and Chen, S.-S. (2019). A comprehensive review of recent developments in 3D printing technique for ceramic membrane fabrication for water purification. *RSC Adv.* 9 (29): 16869–16883. https://doi.org/10.1039/C9RA00872A.

12 Samaei, S.M., Gato-Trinidad, S., and Altaee, A. (2018). The application of pressure-driven ceramic membrane technology for the treatment of industrial wastewaters – a review. *Sep. Purif. Technol.* 200: 198–220. http://www.sciencedirect.com/science/article/pii/S1383586617334123.

13 Gitis, V. and Rothenberg, G. (ed.) (2016). Applications. In: *Ceramic Membranes: New Opportunities and Practical Applications.*, 217–254. Wiley https://doi.org/10.1002/9783527696550.ch4.

14 Weber, R., Chmiel, H., and Mavrov, V. (2003). Characteristics and application of ceramic nanofiltration membranes. *Ann. N. Y. Acad. Sci.* 984 (1): 178–193.

15 Winfield, J., Gajda, I., Greenman, J., and Ieropoulos, I. (2016). A review into the use of ceramics in microbial fuel cells. *Bioresour. Technol.* 215: 296–303. http://www.sciencedirect.com/science/article/pii/S0960852416304382.

16 Chen, X., Chen, T., Li, J. et al. (2019). Ceramic nanofiltration and membrane distillation hybrid membrane processes for the purification and recycling of boric acid from simulative radioactive waste water. *J. Membr. Sci.* 579: 294–301.

17 (2019). Ceramic filter market size, share and trends report ceramic filter market size, share and trends analysis report by application (industrial (bio-filtration, hot gas filtration), residential, commercial), by product (water filter, air filter), and segment. San Francisco, CA 94105, USA, Report ID: 978-1-68038-456-7. p. 124, https://www.grandviewresearch.com/industry-analysis/ceramic-filters-market.

18 Penza, M. (2020). Chapter 12 - Low-cost sensors for outdoor air quality monitoring. In: *Advanced Nanomaterials for Inexpensive Gas Microsensors*, Micro and Nano Technologies (ed. E. Llobet), 235–288. Elsevier http://www.sciencedirect.com/science/article/pii/B9780128148273000128.

19 Tsang, C.H.A., Li, K., Zeng, Y. et al. (2019). Titanium oxide based photocatalytic materials development and their role of in the air pollutants degradation: overview and forecast. *Environ. Int.* 125: 200–228. http://www.sciencedirect.com/science/article/pii/S0160412018329878.

20 Dorey, R.A. (2011). *Ceramic Thick Films for MEMS and Microdevices*, 1e. William Andrew https://www.elsevier.com/books/ceramic-thick-films-for-mems-and-microdevices/dorey/978-1-4377-7817-5.

21 Voskerician, G., Shive, M.S., Shawgo, R.S. et al. (2003). Biocompatibility and biofouling of MEMS drug delivery devices. *Biomaterials* 24 (11): 1959–1967. http://www.sciencedirect.com/science/article/pii/S0142961202005653.

22 Blank, T.A., Eksperiandova, L.P., and Belikov, K.N. (2016). Recent trends of ceramic humidity sensors development: a review. *Sens. Actuators B Chem.* 228: 416–442.

23 Akbar, S., Dutta, P., and Lee, C. (2006). High-temperature ceramic gas sensors: a review. *Int. J. Appl. Ceram. Technol.* 3 (4): 302–311.

24 Feteira, A. (2009). Negative temperature coefficient resistance (NTCR) ceramic thermistors: an industrial perspective. *J. Am. Ceram. Soc.* 92 (5): 967–983.

25 Carter, B. and Norton, G. (2007). *Ceramic Materials Science and Engineering*, 427p. New York: Wiley.

26 Kingery, W.D., Bowen, H.K., and Uhlmann, D.R. *Introduction to Ceramics*, 2e. Wiley.

27 Boch, P. and Baumard, J.-F. (2010). Ceramic compounds: ceramic materials. In: *Ceramic Materials*, 1–28. Wiley https://doi.org/10.1002/9780470612415.ch1.

28 Rahaman, M.N. (ed.) (2003). *Ceramic Processing and Sintering*, 2e. CRC Press.

29 Wessel, J.K. (2004). *Handbook of Advanced Materials - Enabling New Designs* (ed. J.K. Wessel). Wiley-Interscience.

30 Tanzi MC, Farè S, Candiani G. Chapter 1 - Organization, structure, and properties of materials. In: Tanzi MC, Farè S, Candiani G, editors. *Foundations of Biomaterials Engineering*. *Academic Press*; 2019. p. 3–103. http://www.sciencedirect.com/science/article/pii/B9780081010341000013.

31 Osawa, E. (2013). Chapter 2.3 - Nanodiamond—an emerging nano-carbon material. In: *Handbook of Advanced Ceramics (Second Edition)*, 2e (ed. S. Somiya), 89–102. Oxford: Academic Press http://www.sciencedirect.com/science/article/pii/B9780123854698000046.

32 Munro, R.G. and Dapkunas, S.J. (1993). Corrosion characteristics of silicon carbide and silicon nitride. *J. Res. Natl. Inst. Stand. Technol. Res. Natl. Inst. Stand. Technol.* 98 (5): 607–631.

33 Franks, G.V. and Gan, Y. (2007). Charging behavior at the alumina-water interface and implications for ceramic processing. *J. Am. Ceram. Soc.* 90 (11): 3373–3388.

34 Ganguli, D. and Chatterjee, M. (1997). *Ceramic Powder Preparation: A Handbook*. Springer Science+Business Media, LLC.

35 Wefers, K. and Misra, C. (1987). *Oxides and Hydroxides of Aluminum*, Alcoa Technical Paper, 19. http://epsc511.wustl.edu/Aluminum_Oxides_Alcoa1987.pdf.

36 Fierro, J.L.G. (2005). *Metal Oxides: Chemistry and Applications* (ed. F. JLG). CRC Press.

37 Boch, P. and Niepce, J.-C. (2001). *Ceramic Materials - Processes Properties and Applications*. ISTE Ltd.

38 Pezzotti, G. (2014). Bioceramics for hip joints: the Physical Chemistry viewpoint. *Materials (Basel)* 4367–4410.

39 Rezwan, K., Meier, L.P., and Gauckler, L.J. (2005). A prediction method for the isoelectric point of binary protein mixtures of bovine serum albumin and lysozyme adsorbed on colloidal titania and alumina particles. *Langmuir* 21 (8): 3493–3497.

40 Treccani, L., Yvonne Klein, T., Meder, F. et al. (2013). Functionalized ceramics for biomedical, biotechnological and environmental applications. *Acta Biomater.* 9: 7115–7150.

41 Lefèvre, G., Duc, M., Lepeut, P. et al. (2002). Hydration of γ-alumina in water and its effects on surface reactivity. *Langmuir* 18 (20): 7530–7537.

42 Castel, A. (1991). *Les alumines et leurs applications*. Paris: Nathan, DL.

43 Patil, K., Hedge, M., Rattan, T., and Aruna, S. (2008). *Chemistry of Nanocrystalline Oxide Materials - combustion Synthesis, Properties and Applications*. World Scientific Publishing Co. Pte. Ltd.

44 Borges, E.M. (2014). Silica, hybrid silica, hydride silica and non-silica stationary phases for liquid chromatography. *J. Chromatogr. Sci.* 53 (4): 580–597. https://doi.org/10.1093/chromsci/bmu090.

45 Najafpour, G. (2015). *Biochemical Engineering and Biotechnology*, 2e. Elsevier.

46 McGeough, J.A. (2013). *The Engineering of Human Joint Replacements*. Wiley.

47 Attaluri, A.C., Huang, Z., Belwalkar, A. et al. (2009). Evaluation of nano-porous alumina membranes for hemodialysis application. *ASAIO J.* 55 (3): 217–223.

48 Ismail, A.F. and Matsuura, T. (2016). *Membrane Technology for Water and Wastewater Treatment, Energy and Environment*. CRC Press.

49 Lee, W., Ji, R., Gosele, U., and Nielsch, K. (2006). Fast fabrication of long-range ordered porous alumina membranes by hard anodization. *Nat. Mater.* 5 (9): 741–747.

50 Sedel, L. (2000). Evolution of alumina-on-alumina implants: a review. *Clin. Orthop. Relat. Res.* 379: 48–54.

51 Boyer, P., Huten, D., Loriaut, P. et al. (2010). Is alumina-on-alumina ceramic bearings total hip replacement the right choice in patients younger than 50 years of age? A 7- to 15-year follow-up study. *Orthop. Traumatol. Surg. Res.* 96 (6): 616–622.

52 Kurtz, S.M., Kocagöz, S., Arnholt, C. et al. (2014). Advances in zirconia toughened alumina biomaterials for total joint replacement. *J. Mech. Behav. Biomed. Mater.* 31: 107–116.

53 Faramawy, S., El-Naggar, A.Y., El-Fadly, A.M. et al. (2016). Silica, alumina and aluminosilicates as solid stationary phases in gas chromatography. *Arab. J. Chem.* 9 (Suppl): S765–S775.

54 Buchberger, W. and Winsauer, K. (1989). Alumina as stationary phase for ion chromatography and column-coupling techniques. *J. Chromatogr. A* 482 (2): 401–406.

55 Aw, M.S., Bariana, M., and Losic, D. (2015). Nanoporous anodic alumina for drug delivery and biomedical applications. In: *Nanoporous Alumina: Fabrication, Structure, Properties and Applications* (ed. D. Losic and A. Santos), 319–354. Cham: Springer International Publishing.

56 Porta-i-Batalla, M., Eckstein, C., Xifré-Pérez, E. et al. (2016). Sustained, controlled and stimuli-responsive drug release systems based on nanoporous anodic alumina with layer-by-layer polyelectrolyte. *Nanoscale Res. Lett.* 11: 372.

57 Toccafondi, C., Thorat, S., La Rocca, R. et al. (2014). Multifunctional substrates of thin porous alumina for cell biosensors. *J. Mater. Sci. Mater. Med.* 25 (10): 2411–2420.

58 Dong, L., Yang, H., Liu, S. et al. (2015). Fabrication and anti-biofouling properties of alumina and zeolite nanoparticle embedded ultrafiltration membranes. *Desalination* 365: 70–78.

59 Wang, F., Lee, J., Ha, J.-H., and Song, I.-H. (2017). Surface modification of alumina membranes via a sol-gel process for antifouling properties. *Mater. Lett.* 191: 200–202.

60 Ahmad, R., Kim, J.K., Kim, J.H., and Kim, J. (2017). Well-organized, mesoporous nanocrystalline TiO2 on alumina membranes with hierarchical architecture: antifouling and photocatalytic activities. *Catal. Today* 282, Part:: 2–12.

61 Mauter, M.S., Wang, Y., Okemgbo, K.C. et al. (2011). Antifouling ultrafiltration membranes via post-fabrication grafting of biocidal nanomaterials. *ACS Appl. Mater. Interfaces* 3 (8): 2861–2868.

62 Eranna, G. (2019). *Metal Oxide Nanostructures as Gas Sensing Devices*. CRC Press.

63 Kocanda, M., Haji-Sheikh, M.J., and Ballantine, D.S. (2009). Detection of cyclic volatile organic compounds using single-step anodized nanoporous alumina sensors. *IEEE Sens. J.* 9 (7): 836–841.

64 Khataee, A. and Mansoori, A.G. (2011). *Nanostructured Titanium Dioxide Materials Properties, Preparation and Applications*. World Scientific Publishing Co Pte Ltd.

65 Di Paola, A., Bellardita, M., and Palmisano, L. (2013). Brookite, the least known TiO_2 photocatalyst. *Catalysts* 3: 36–73.

66 Carpenter, M.A. and Mathur, S. (2013). *Metal Oxide Nanomaterials for Chemical Sensors* (ed. A. Kolmakov). Springer.

67 Schmidt, J. and Vogelsberger, W. (2006). Dissolution kinetics of titanium dioxide nanoparticles: the observation of an unusual kinetic size effect. *J. Phys. Chem. B* 110 (9): 3955–3963.

68 Marchand, R., Brohan, L., and Tournoux, M. (1980). TiO_2(B) a new form of titanium dioxide and the potassium octatitanate $K_2Ti_8O_{17}$. *Mater. Res. Bull.* 15 (8): 1129–1133.

69 Nowotny, J. (2011). *Oxide Semiconductors for Solar Energy Conversion Titanium Dioxide*, 1e. CRC Press.

70 Esch, T.R., Gadaczek, I., and Bredow, T. (2014). Surface structures and thermodynamics of low-index of rutile, brookite and anatase – a comparative DFT study. *Appl. Surf. Sci.* 288: 275–287.

71 Gouma, P.-I. (2010). *Nanomaterials for Chemical Sensors and Biotechnology*, 1e. Taylor & Francis.

72 Bourikas, K., Kordulis, C., and Lycourghiotis, A. (2014). Titanium dioxide (anatase and rutile): Surface chemistry, liquid -solid interface chemistry, and scientific synthesis of supported catalysts. *Chem. Rev.* 114 (19): 9754–9823.

73 Fornabaio, M., Palmero, P., Traverso, R. et al. (2015). Zirconia-based composites for biomedical applications: role of second phases on composition, microstructure and zirconia transformability. *J. Eur. Ceram. Soc.* 35 (14): 4039–4049.

74 Kosmulski, M. (2016). Isoelectric points and points of zero charge of metal (hydr)oxides: 50 years after Parks' review. *Adv. Colloid Interface Sci.* 238: 1–61.

75 Derr, L., Dringen, R., Treccani, L. et al. (2015). Physisorption of enzymatically active chymotrypsin on titania colloidal particles. *J. Colloid Interface Sci.* 455.

76 Borghi, F., Vyas, V., Podestà, A., and Milani, P. (2013). Nanoscale roughness and morphology affect the isoelectric point of titania surfaces. *PLoS One* 8 (7): e68655.

77 Schmidt, J. and Vogelsberger, W. (2009). Aqueous long-term solubility of titania nanoparticles and titanium(IV) hydrolysis in a sodium chloride system studied by adsorptive stripping voltammetry. *J. Sol. Chem.* 38 (10): 1267–1282.

78 Ziemniak, S.E., Jones, M.E., and Combs, K.E.S. (1993). Solubility behavior of titanium(IV) oxide in alkaline media at elevated temperatures. *J. Sol. Chem.* 22 (7): 601–623.

79 Ohama, Y. and Van Gemert, D. (2011). *Application of Titanium Dioxide Photocatalysis to Construction Materials* (ed. Y. Ohama and D. Van Gemert). Springer.

80 Fujishima, X. and Honda, X. (1972). Electrochemical photolysis of water at a semiconductor electrode. *Nature* 238 (5358): 37–38. https://link.springer.com/book/10.1007/978-94-007-1297-3.

81 Li, L., Yan, J., Wang, T. et al. (2015). Sub-10 nm rutile titanium dioxide nanoparticles for efficient visible-light-driven photocatalytic hydrogen production. *Nat. Commun.* 6: 5881.

82 Inerbaev, T., Hoefelmeyer, J.D., and Kilin, D.S. (2013). Photoinduced charge transfer from titania to surface doping site. *J. Phys. Chem. C Nanomater. Interfaces* 117 (19): 9673–9692.

83 Bora, D.K., Rozhkova, E.A., Schrantz, K. et al. (2012). Functionalization of nanostructured hematite thin-film electrodes with the light-harvesting membrane protein C-phycocyanin yields an enhanced photocurrent. *Adv. Funct. Mater.* 22 (3): 490–502.

84 Sardar, S., Sarkar, S., Myint, M.T.Z. et al. (2013). Role of central metal ions in hematoporphyrin-functionalized titania in solar energy conversion dynamics. *Phys. Chem. Chem. Phys.* 15 (42): 18562–18570.

85 Bai, J. and Zhou, B. (2014 Oct). Titanium dioxide nanomaterials for sensor applications. *Chem. Rev.* 114 (19): 10131–10176.

86 Fanun, M. (2011). *Colloids in Biotechnology*, 1e. CRC Press.

87 Tan, J., Li, R., and Jiang, Z.-T. (2014 Dec). Discrimination of fresh fruit juices by a fluorescent sensor array for carboxylic acids based on molecularly imprinted titania. *Food Chem.* 165: 35–41.

88 Morosanova, M.A. and Morosanova, E.I. (2016). A silica-titania sensor material prepared by cetylpyridinium chloride assisted sol-gel synthesis for solid phase spectrophotometric and visual test determination of propyl gallate in food samples. *Anal. Methods* 8 (45): 8092–8098.

89 Hesjedal, D.V.R., Burek, M.J., Iutzi, R.M. et al. (2011). Development of an electronic nose sensing platform for undergraduate education in nanotechnology. *Eur. J. Phys.* 32 (3): 675.

90 Righettoni, M., Amann, A., and Pratsinis, S.E. (2015). Breath analysis by nanostructured metal oxides as chemo-resistive gas sensors. *Mater. Today* 18 (3): 163–171.

91 Lee, J., Kim, D.H., Hong, S.-H., and Jho, J.Y. (2011). A hydrogen gas sensor employing vertically aligned TiO2 nanotube arrays prepared by template-assisted method. *Sens. Actuators B Chem.* 160 (1): 1494–1498.

92 Varghese, O., Mor, G., Grimes, C. et al. (2004). A titania nanotube-array room-temperature sensor for selective detection of hydrogen at low concentrations. *J. Nanosci. Nanotechnol.* 4 (7): 733–737.

93 Du, L.X., Jiang, Z.T., and Li, R. (2013). Preparation of porous titania microspheres for HPLC packing by sol-gel method. *Mater. Lett.* 95: 17–20.

94 Wei, J., Jiang, Z.-T., Li, R., and Tan, J. (2012). Preparation of titania monolith column and application in determination of benzoic acid by HILIC. *Chromatographia* 75 (11): 563–569.

95 Winkler, J. and Marmé, S. (2000). Titania as a sorbent in normal-phase liquid chromatography. *J. Chromatogr. A* 888 (1–2): 51–62.

96 Abi Jaoudé, M. and Randon, J. (2011). Capillary monolithic titania column for miniaturized liquid chromatography and extraction of organo-phosphorous compounds. *Anal. Bioanal. Chem.* 1241–1249.

97 Abd El-Ghany, O.S. and Sherief, A.H. (2016). Zirconia based ceramics, some clinical and biological aspects: Review. *Futur. Dent. J.* 2 (2): 55–64.

98 Chen, Y.-W., Moussi, J., Drury, J.L., and Wataha, J.C. (2016). Zirconia in biomedical applications. *Expert Rev. Med. Devices* 13 (10): 945–963.

99 Tang, S., Huang, X., Chen, X., and Zheng, N. (2010). Hollow mesoporous zirconia nanocapsules for drug delivery. *Adv. Funct. Mater.* 20 (15): 2442–2447.

100 Polyak, A., Naszalyi Nagy, L., Mihaly, J. et al. (2017). Preparation and 68Ga-radiolabeling of porous zirconia nanoparticle platform for PET/CT-imaging guided drug delivery. *J. Pharm. Biomed. Anal.* 137: 146–150.

101 Catauro, M., Raucci, M., and Ausanio, G. (2008). Sol-gel processing of drug delivery zirconia/polycaprolactone hybrid materials. *J. Mater. Sci. Mater. Med.* 19 (2): 531–540.

102 Kumar, S., Kumar, S., Tiwari, S. et al. (2015). Biofunctionalized nanostructured zirconia for biomedical application: a smart approach for oral cancer detection. *Adv. Sci.*

103 Ahmad, N.M., Abdullah, J., Yusof, N.A. et al. (2016). Amperometric biosensor based on zirconium oxide/polyethylene glycol/tyrosinase composite film for the detection of phenolic compounds. *Biosensors* 6 (3): 31–44.

104 Skinner, S.J. and Kilner, J.A. (2003). Oxygen ion conductors. *Mater. Today* 6 (3): 30–37.

105 Durá, O.J., López De La Torre, M.A., Vázquez, L. et al. (2010). Ionic conductivity of nanocrystalline yttria-stabilized zirconia: Grain boundary and size effects. *Phys. Rev. B – Condens. Matter Mater. Phys.* 81 (18).

106 Elm, M.T., Hofmann, J.D., Suchomski, C. et al. (2015). Ionic conductivity of mesostructured yttria-stabilized zirconia thin films with cubic pore symmetry - on the influence of water on the surface oxygen ion transport. *ACS Appl. Mater. Interfaces* 7 (22): 11792–11801.

107 Lai, A., Du, Z., Gan, C.L., and Schuh, C.A. (2013). Shape memory and superelastic ceramics at small scales. *Science (80)* 341 (6153): 1505 LP–1508.

108 Wang, J. and Stevens, R. (1989). Zirconia-toughened alumina (ZTA) ceramics. *J. Mater. Sci.* 24: 3421–3440.

109 De Aza, A.H., Chevalier, J., Fantozzi, G. et al. (2002). Crack growth resistance of alumina, zirconia and zirconia toughened alumina ceramics for joint prostheses. *Biomaterials* 23 (3): 937–945.

110 Garvie, R.C., Hannink, R.H., and Pascoe, R.T. (1975). Ceramic steel? *Nature* 258 (5537): 703–704.

111 Yong, Z. (1992). *Zirconia MMR*. Elsevier.

112 Hannink, R.H.J., Kelly, P.M., and Muddle, B.C. (2000). Transformation toughening in zirconia-containing ceramics. *J. Am. Ceram. Soc.* 83 (3): 461–487.

113 Qiu, L., Guzonas, D.A., and Webb, D.G. (2009). Zirconium dioxide solubility in high temperature aqueous solutions. *J. Sol. Chem.* 38 (7): 857–867.

114 Nawrocki, J., Rigney, M., McCormick, A., and Carr, P.W. (1993). Chemistry of zirconia and its use in chromatography. *J. Chromatogr. A* 657: 229–282.

115 Kephart, T.S. and Dasgupta, P.K. (2000). Hot eluent capillary liquid chromatography using zirconia and titania based stationary phases. *Anal. Chim. Acta* 414 (1–2): 71–78.

116 Sanagi, M.M., See, H.H., Ibrahim, W.A.W., and Naim, A.A. (2004). High temperature liquid chromatography of triazole fungicides on polybutadiene-coated zirconia stationary phase. *J. Chromatogr. A* 1059 (1–2): 95–101.

117 Dunlap, C.J., Carr, P.W., McNeff, C.V., and Stoll, D. (2001). Peer reviewed: zirconia stationary phases for extreme separations. *Anal. Chem.* 73 (21): 598 A–607 A.

118 Naszályi Nagy, L., Mihály, J., Polyak, A. et al. (2015). Inherently fluorescent and porous zirconia colloids: preparation, characterization and drug adsorption studies. *J. Mater. Chem. B* 3 (3): 7529–7537.

119 Shackelford, J.F. and Doremus, R.H. (ed.) (2008). *Ceramic and Glass Materials*. Boston, MA: Springer.

120 Martin, K.R. (2007). The chemistry of silica and its potential health benefits. *J. Nutr. Health Aging* 11 (2): 94–97.

121 Will, J., Gerhardt, L.-C., and Boccaccini, A.R. (2012). Bioactive glass-based scaffolds for bone tissue engineering. In: *Tissue Engineering III: Cell - Surface Interactions for Tissue Culture* (ed. C. Kasper, F. Witte and R. Pörtner), 195–226. Berlin, Heidelberg: Springer Berlin Heidelberg https://doi.org/10.1007/10_2011_106.

122 Martins, T.B., Burlingame, R., von Mühlen, C.A. et al. (2004). Evaluation of multiplexed fluorescent microsphere immunoassay for detection of autoantibodies to nuclear antigens. *Clin. Diagn. Lab Immunol.* 11 (6): 1054–1059.

123 Vallet-Regi, M. and Balas, F. (2008). Silica materials for medical applications. *Open Biomed. Eng. J.* 2: 1–9.

124 Lakshtanov, D.L., Sinogeikin, S.V., and Bass, J.D. (2007). High-temperature phase transitions and elasticity of silica polymorphs. *Phys. Chem. Miner.* 34 (1): 11–22. https://doi.org/10.1007/s00269-006-0113-y.

125 Lenher, V. and Merrill, H.B. (1917). The solubility of silica. *J. Am. Chem. Soc.* 39 (12): 2630–2638. https://doi.org/10.1021/ja02257a013.

126 Mitra, A. and Rimstidt, J.D. (2009). Solubility and dissolution rate of silica in acid fluoride solutions. *Geochim. Cosmochim. Acta* 73 (23): 7045–7059. http://www.sciencedirect.com/science/article/pii/S0016703709005389.

127 Mitsyuk, B.M. (1984). Mechanism of silica dissolution and state of silicic acid in hydrothermal solutions. *Theor. Exp. Chem.* 19 (5): 554–559. https://doi.org/10.1007/BF00526030.

128 Nibori, Y., Kunita, M., Tochiyama, O., and Chida, T. (2000). Dissolution rates of amorphous silica in highly alkaline solution. *J. Nucl. Sci. Technol.* 37 (4): 349–357. https://doi.org/10.1080/18811248.2000.9714905.

129 Pagliaro, M. (2009). *Silica-Based Materials for Advanced Chemical Applications*. RSC.

130 Kresge, C.T., Leonowicz, M.E., Roth, W.J. et al. (1992). Ordered mesoporous molecular sieves synthesized by a liquid-crystal template mechanism. *Nature* 359 (6397): 710–712.

131 Trewyn, B.G., Slowing, I.I., Giri, S. et al. (2007). Synthesis and functionalization of a mesoporous silica nanoparticle based on the sol-gel process and applications in controlled release. *Acc. Chem. Res.* 40 (9): 846–853.

132 Laskowski, Ł., Laskowska, M., Bałanda, M. et al. (2014). Mesoporous silica SBA-15 functionalized by nickel–phosphonic units: Raman and magnetic analysis. *Micropor. Mesopor. Mater.* 200: 253–259.

133 Gibson, L.T. (2014). Mesosilica materials and organic pollutant adsorption: part A removal from air. *Chem. Soc. Rev.* 43 (15): 5163–5172.

134 Qiu, H., Liang, X., Sun, M., and Jiang, S. (2011). Development of silica-based stationary phases for high-performance liquid chromatography. *Anal. Bioanal. Chem.* 399 (10): 3307–3322. https://doi.org/10.1007/s00216-010-4611-x.

135 Tanaka, N., Kobayashi, H., Ishizuka, N. et al. (2002). Monolithic silica columns for high-efficiency chromatographic separations. *J. Chromatogr. A* 965 (1): 35–49. http://www.sciencedirect.com/science/article/pii/S0021967301015825.

136 Liberman, A., Mendez, N., Trogler, W.C., and Kummel, A.C. (2014 Sep). Synthesis and surface functionalization of silica nanoparticles for nanomedicine. *Surf. Sci. Rep.* 69 (2–3): 132–158. https://pubmed.ncbi.nlm.nih.gov/25364083.

137 Ghosh, S. (2019). Chapter 9 - Mesoporous silica-based nano drug-delivery system synthesis, characterization, and applications. In: *Micro and Nano Technologies* (ed. S.S. Mohapatra, S. Ranjan, N. Dasgupta, et al.), 285–317. Elsevier http://www.sciencedirect.com/science/article/pii/B9780128140338000096.

138 Pednekar PP, Godiyal SC, Jadhav KR, Kadam VJ. Chapter 23 - Mesoporous silica nanoparticles: a promising multifunctional drug delivery system. In: Ficai A, Grumezescu AMBT-N for CT, editors. *Micro and Nano Technologies Elsevier*; 2017. p. 593–621. http://www.sciencedirect.com/science/article/pii/B9780323461443000234.

139 Zhang, Y. and Xu, J. (2020). Mesoporous silica nanoparticle-based intelligent drug delivery system for bienzyme-responsive tumour targeting and controlled release. *R. Soc. Open Sci.* 5 (1): 170986. https://doi.org/10.1098/rsos.170986.

140 Cheng, Y.-J., Qin, S.-Y., Ma, Y.-H. et al. (2019). Super-pH-sensitive mesoporous silica nanoparticle-based drug delivery system for effective combination cancer therapy. *ACS Biomater. Sci. Eng.* 5 (4): 1878–1886. https://doi.org/10.1021/acsbiomaterials.9b00099.

141 Manzano, M. and Vallet-Regí, M. (2020). Mesoporous silica nanoparticles for drug delivery. *Adv. Funct. Mater.* 30 (2): 1902634. https://doi.org/10.1002/adfm.201902634.

142 Tang, F., Li, L., and Chen, D. (2012). Mesoporous silica nanoparticles: synthesis, biocompatibility and drug delivery. *Adv. Mater.* 24 (12): 1504–1534. https://doi.org/10.1002/adma.201104763.

143 Sun, B., Zhou, G., and Zhang, H. (2016). Synthesis, functionalization, and applications of morphology-controllable silica-based nanostructures: a review. *Prog. Solid State Chem.* 44 (1): 1–19. http://www.sciencedirect.com/science/article/pii/S0079678616000029.

144 Argyo, C., Weiss, V., Bräuchle, C., and Bein, T. (2014). Multifunctional mesoporous silica nanoparticles as a universal platform for drug delivery. *Chem. Mater.* 26 (1): 435–451.

145 Caltagirone, C., Bettoschi, A., Garau, A., and Montis, R. (2015). Silica-based nanoparticles: a versatile tool for the development of efficient imaging agents. *Chem. Soc. Rev.* 44 (14): 4645–4671. https://doi.org/10.1039/C4CS00270A.

146 Yu, L., Lin, H., Lu, X., and Chen, Y. (2018). Multifunctional mesoporous silica nanoprobes: Material chemistry-based fabrication and bio-imaging functionality. *Adv. Ther.* 1 (8): 1800078. https://doi.org/10.1002/adtp.201800078.

147 Shahabi, S., Treccani, L., Dringen, R., and Rezwan, K. (2015). Modulation of silica nanoparticle uptake into human osteoblast cells by variation of the ratio of amino and sulfonate surface groups: effects of serum. *ACS Appl. Mater. Interfaces* 7 (25):

13821–13833. http://www.pubmedcentral.nih.gov/articlerender.fcgi?artid=4490775&tool=pmcentrez&rendertype=abstract.

148 Shahabi, S., Döscher, S., Bollhorst, T. et al. (2015). Enhancing cellular uptake and doxorubicin delivery of mesoporous silica nanoparticles via surface functionalization: effects of serum. *ACS Appl. Mater. Interfaces* 7 (48): 26880–26891. https://doi.org/10.1021/acsami.5b09483.

149 Shahabi, S., Treccani, L., Dringen, R., and Rezwan, K. (2015). Dual fluorophore doped silica nanoparticles for cellular localization studies in multiple stained cells. *Acta Biomater.* 14: 208–216.

150 Shahabi, S., Treccani, L., and Rezwan, K. (2016). A comparative study of three different synthesis routes for hydrophilic fluorophore-doped silica nanoparticles. *J. Nanoparticle Res.* 18 (1): 28.

151 Shahabi, S., Treccani, L., and Rezwan, K. (2015). Amino acid-catalyzed seed regrowth synthesis of photostable high fluorescent silica nanoparticles with tunable sizes for intracellular studies. *J. Nanoparticle Res.* 17 (6): https://doi.org/10.1007/s11051-015-3072-8.

152 Hartmann, M. and Kostrov, X. (2013). Immobilization of enzymes on porous silicas – benefits and challenges. *Chem. Soc. Rev.* 42 (15): 6277–6289. https://doi.org/10.1039/C3CS60021A.

153 Carlsson, N., Gustafsson, H., Thörn, C. et al. (2014). Enzymes immobilized in mesoporous silica: a physical–chemical perspective. *Adv. Colloid Interface Sci.* 205: 339–360.

154 Hou, C., Ghéczy, N., Messmer, D. et al. (2019). Stable immobilization of enzymes in a macro- and mesoporous silica monolith. *ACS Omega* 4 (4): 7795–7806. https://doi.org/10.1021/acsomega.9b00286.

155 Ortiz-Martínez, K., Vargas-Valentín, D.A., and Hernández-Maldonado, A.J. (2018). Adsorption of contaminants of emerging concern from aqueous solutions using Cu^{2+} amino grafted SBA-15 mesoporous silica: multicomponent and metabolites adsorption. *Ind. Eng. Chem. Res.* 57 (18): 6426–6439. https://doi.org/10.1021/acs.iecr.7b05168.

156 Dikio, E. (2018). Silica-based mesoporous materials; emerging designer adsorbents for aqueous pollutants removal and water treatment. *Micropor. Mesopor. Mater.* 1: 266.

157 Saxena, R., Saxena, M., and Lochab, A. (2020). Recent progress in nanomaterials for adsorptive removal of organic contaminants from wastewater. *ChemistrySelect* 5 (1): 335–353. https://doi.org/10.1002/slct.201903542.

158 Cashin, V.B., Eldridge, D.S., Yu, A., and Zhao, D. (2018). Surface functionalization and manipulation of mesoporous silica adsorbents for improved removal of pollutants: a review. *Environ. Sci. Water Res. Technol.* 4 (2): 110–128. https://doi.org/10.1039/C7EW00322F.

159 Zusman, R., Rottman, C., Ottolenghi, M., and Avnir, D. (1990). Doped sol-gel glasses as chemical sensors. *J. Non Cryst. Solids* 122 (1): 107–109. http://www.sciencedirect.com/science/article/pii/002230939090232B.

160 Wolfbeis, O.S., Reisfeld, R., and Oehme, I. (1996). Sol-gels and chemical sensors. In: *Optical and Electronic Phenomena in Sol-Gel Glasses and Modern Application. Structure and Bonding*, vol. 85. Berlin, Heidelberg: Springer https://doi.org/10.1007/BFb0111488.

161 Barczak, M., McDonagh, C., and Wencel, D. (2016). Micro- and nanostructured sol-gel-based materials for optical chemical sensing (2005–2015). *Microchim. Acta* 183 (7): 2085–2109. https://doi.org/10.1007/s00604-016-1863-y.

162 McDonagh, C., Burke, C.S., and MacCraith, B.D. (2008). Optical chemical sensors. *Chem. Rev.* 108 (2): 400–422. https://doi.org/10.1021/cr068102g.

163 Hazra, S. and Ghosh, N. (2014). Preparation of nanoferrites and their applications. *J. Nanosci. Nanotechnol.* 2: 1983–2000.

164 Revia, R.A. and Zhang, M. (2016). Magnetite nanoparticles for cancer diagnosis, treatment, and treatment monitoring: recent advances. *Mater Today.* 19 (3): 157–168.

165 Dinali, R., Ebrahiminezhad, A., Manley-Harris, M. et al. (2017 Jan). Iron oxide nanoparticles in modern microbiology and biotechnology. *Crit. Rev. Microbiol.* 1–15.

166 Gupta, A.K. and Gupta, M. (2005). Synthesis and surface engineering of iron oxide nanoparticles for biomedical applications. *Biomaterials* 26 (18): 3995–4021.

167 Huber, D.L. (2005). Synthesis, properties, and applications of iron nanoparticles. *Small* 1 (5): 482–501.

168 Lee, N., Yoo, D., Ling, D. et al. (2015). Iron oxide based nanoparticles for multimodal imaging and magnetoresponsive therapy. *Chem. Rev.* 115 (19): 10637–10689.

169 Munro, C.D. and Plucknett, K.P. (2010). Colloidal characterization and aqueous gel casting of barium titanate ceramics. In: *Innovative Processing and Manufacturing of Advanced Ceramics and Composites: Ceramic Transactions* (ed. Z.A. Munir, T. Ohji, Y. Hotta and M. Singh), 215–226. Wiley.

170 Genchi, G.G., Marino, A., Rocca, A. et al. (2016). Barium titanate nanoparticles: promising multitasking vectors in nanomedicine. *Nanotechnology* 27 (23): 232001. https://doi.org/10.1088/0957-4484/27/2/232001.

171 Ciofani, G., Danti, S., Ricotti, L. et al. (2010). Potential applications of barium titanate nanoparticles in nanomedicine: a preliminary study. In: *2010 10th IEEE Conf Nanotechnology, NANO 2010*, 987–990.

172 Acosta, M., Novak, N., Rojas, V. et al. (2017). BaTiO3-based piezoelectrics: fundamentals, current status, and perspectives. *Appl. Phys. Rev.* 4 (4): 41305. https://doi.org/10.1063/1.4990046.

173 Tang, Y., Wu, C., Wu, Z. et al. (2017). Fabrication and in vitro biological properties of piezoelectric bioceramics for bone regeneration. *Sci. Rep.* 7 (1): 43360. https://doi.org/10.1038/srep43360.

174 Bowland, C.C., Malakooti, M.H., and Sodano, H.A. (2017 Feb). Barium titanate film interfaces for hybrid composite energy harvesters. *ACS Appl. Mater. Interfaces* 9 (4): 4057–4065.

175 Koka, A. and Sodano, H.A. (2013). High-sensitivity accelerometer composed of ultra-long vertically aligned barium titanate nanowire arrays. *Nat. Commun.* 4: 2682.

176 Heinrich, J.G. and Gomes, C.M. (2000). *Introduction to Ceramics Processing*. TU Cluasthal.

177 Ciarlo, D.R. (2002). Silicon nitride thin windows for biomedical microdevices. *Biomed. Microdev.* 4 (1): 63–68.

178 Ring, E., Peckys, D.B., Dukes, M.J. et al. (2011). Silicon nitride windows for electron microscopy of whole cells. *J. Microsc.* 243: 273–283.

179 Jenison, R., Yang, S., Haeberli, A., and Polisky, B. (2001). Interference-based detection of nucleic acid targets on optically coated silicon. *Nat. Biotechnol.* 19 (1): 62–65.

180 Rahaman, N. and Xiao, W. (2017 Nov). Silicon nitride bioceramics in healthcare. *Int. J. Appl. Ceram. Technol.* 24: 15.

181 Lal, S., Caseley, E.A., Hall, R.M., and Tipper, J.L. (2018). Biological impact of silicon nitride for orthopaedic applications: role of particle size, surface composition and donor variation. *Sci. Rep.* 8 (1): 9109. https://doi.org/10.1038/s41598-018-27494-y.

182 Pezzotti, G., Marin, E., Adachi, T. et al. (2017). Bioactive silicon nitride: a new therapeutic material for osteoarthropathy. *Sci. Rep.* 7 (1): 44848. https://doi.org/10.1038/srep44848.

183 Zanocco, M., Boschetto, F., Zhu, W. et al. (2020). 3D-additive deposition of an antibacterial and osteogenic silicon nitride coating on orthopaedic titanium substrate. *J. Mech. Behav. Biomed. Mater.* 103: 103557. http://www.sciencedirect.com/science/article/pii/S1751616119309099.

184 Saddow, S.E., Locke, C.W., Severino, A. et al. (2016). Silicon carbide biotechnology. In: *Silicon Carbide Biotechnology*, 2e, 17–61. Elsevier.

185 Will, J., Hoppe, A., Müller, F.A. et al. (2010). Bioactivation of biomorphous silicon carbide bone implants. *Acta Biomater.* 6 (12): 4488–4494. http://www.sciencedirect.com/science/article/pii/S1742706110003028.

186 Gryshkov, O., Klyui, N.I., Temchenko, V.P. et al. (2016). Porous biomorphic silicon carbide ceramics coated with hydroxyapatite as prospective materials for bone implants. *Mater. Sci. Eng. C* 68: 143–152. http://www.sciencedirect.com/science/article/pii/S0928493116305458.

187 Gabriel, G., Erill, I., Caro, J. et al. (2007). Manufacturing and full characterization of silicon carbide-based multi-sensor micro-probes for biomedical applications. *Microelectron. J.* 38 (3): 406–415. http://www.sciencedirect.com/science/article/pii/S002626920600276X.

188 Cao, Y., Dong, H., Pu, S., and Zhang, X. (2018). Photoluminescent two-dimensional SiC quantum dots for cellular imaging and transport. *Nano Res.* 11 (8): 4074–4081. https://doi.org/10.1007/s12274-018-1990-3.

189 Beke, D., Szekrényes, Z., Czigány, Z. et al. (2015). Dominant luminescence is not due to quantum confinement in molecular-sized silicon carbide nanocrystals. *Nanoscale* 7 (25): 10982–10988. https://doi.org/10.1039/C5NR01204J.

190 Botsoa, J., Lysenko, V., Alain, G. et al. (2008). Application of 3C-SiC quantum dots for living cell imaging. *Appl. Phys. Lett.* 92: 173902.

191 Mortensen, M.W., Björkdahl, O., Sørensen, P.G. et al. (2006). Functionalization and cellular uptake of boron carbide nanoparticles. The first step toward T cell-guided boron neutron capture therapy. *Bioconjug. Chem.* 17 (2): 284–290. https://doi.org/10.1021/bc050206v.

192 Vallet-Regi, M., Garcia, M.M., and Colilla, M. (2013). *Biomedical Applications of Mesoporous Ceramics: Drug Delivery, Smart Materials, and Bone Tissue Engineering*. CRC Press.

193 Jain, K.K. (2014). *Applications of Biotechnology in Oncology*. Humana Press https://www.springer.com/gp/book/9781461492443.

194 Kawalec, J.S. (2001). Carbon in biomedical engineering. In: *Encyclopedia of Materials: Science and Technology* (ed. B. KHJ, R.W. Cahn, M.C. Flemings, et al.), 922–926. Oxford: Elsevier http://www.sciencedirect.com/science/article/pii/B0080431526001765.

195 Gupta, S. and Tai, N.-H. (2016). Carbon materials as oil sorbents: a review on the synthesis and performance. *J. Mater. Chem. A* 4 (5): 1550–1565. https://doi.org/10.1039/C5TA08321D.

196 Mendes, D.G., Iusim, M., Angel, D. et al. (1986). Ligament and tendon substitution with composite carbon fiber strands. *J. Biomed. Mater. Res.* 20 (6): 699–708. https://doi.org/10.1002/jbm.820200604.

197 Goodarzi, S., Da Ros, T., Conde, J. et al. (2017). Fullerene: biomedical engineers get to revisit an old friend. *Mater. Today* 20 (8): 460–480. http://www.sciencedirect.com/science/article/pii/S1369702116301808.

198 Bakry, R., Vallant, R.M., Najam-ul-Haq, M. et al. (2007). Medicinal applications of fullerenes. *Int. J. Nanomed.* 2 (4): 639–649. https://pubmed.ncbi.nlm.nih.gov/18203430.

199 Castro, E., Hernandez Garcia, A., Zavala, G., and Echegoyen, L. (2017). Fullerenes in biology and medicine. *J. Mater. Chem. B* 5 (32): 6523–6535. https://pubmed.ncbi.nlm.nih.gov/29225883.

200 Samal, S. and Geckeler, K.E. (2000). Cyclodextrin–fullerenes: a new class of water-soluble fullerenes. *Chem. Commun.* (13): 1101–1102. https://doi.org/10.1039/B000710M.

201 Bolskar, R.D. (2012). *Fullerenes for Drug Delivery BT - Encyclopedia of Nanotechnology* (ed. B. Bhushan), 898–911. Dordrecht: Springer Netherlands https://doi.org/10.1007/978-90-481-9751-4_76.

202 Fabbro, A., Bosi, S., Ballerini, L., and Prato, M. (2012). Carbon nanotubes: artificial nanomaterials to engineer single neurons and neuronal networks. *ACS Chem. Neurosci.* 3 (8): 611–618. https://pubmed.ncbi.nlm.nih.gov/22896805.

203 Veetil, J.V. and Ye, K. (2009). Tailored carbon nanotubes for tissue engineering applications. *Biotechnol. Prog.* 25 (3): 709–721. https://pubmed.ncbi.nlm.nih.gov/19496152.

204 Oprych, K.M., Whitby, R.L.D., Mikhalovsky, S.V. et al. (2016). Repairing peripheral nerves: is there a role for carbon nanotubes? *Adv. Healthc. Mater.* 5 (11): 1253–1271. https://doi.org/10.1002/adhm.201500864.

205 Singh, R. and Torti, S.V. (2013). Carbon nanotubes in hyperthermia therapy. *Adv. Drug Deliv. Rev.* 65 (15): 2045–2060. http://www.sciencedirect.com/science/article/pii/S0169409X13001841.

206 Adeli, M., Soleyman, R., Beiranvand, Z., and Madani, F. (2013). Carbon nanotubes in cancer therapy: a more precise look at the role of carbon nanotube–polymer interactions. *Chem. Soc. Rev.* 42 (12): 5231–5256. https://doi.org/10.1039/C3CS35431H.

207 Kaur J, Gill GS, Jeet K. Chapter 5 - Applications of carbon nanotubes in drug delivery: a comprehensive review. In: Mohapatra SS, Ranjan S, Dasgupta N, Mishra RK, Thomas SBT-C and B of N for DD, editors. *Micro and Nano Technologies. Elsevier*; 2019. p. 113–35. http://www.sciencedirect.com/science/article/pii/B9780128140314000052.

208 Zhang, W., Zhang, Z., and Zhang, Y. (2011). The application of carbon nanotubes in target drug delivery systems for cancer therapies. *Nanoscale Res. Lett.* 6 (1): 555. https://pubmed.ncbi.nlm.nih.gov/21995320.

209 Tiwari, A. and APF, T. (ed.) (2014). *Biosensors Nanotechnology*. Wiley.

210 Vallet-Regi, M. (ed.) (2014). *Bio-Ceramics with Clinical Applications*. Wiley.

211 Vallet-Regi, M., Manzano Garcìa, M., and Colilla, M. (2012). *Biomedical Applications of Mesoporous Ceramics: Drug Delivery, Smart Materials and Bone Tissue Engineering*, 1e. CRC Press.

212 Zhang, M., Liao, C., Mak, C.H. et al. (2015). Highly sensitive glucose sensors based on enzyme-modified whole-graphene solution-gated transistors. *Sci. Rep.* 5: 8311.

213 Zhang, R. and Chen, W. (2017). Recent advances in graphene-based nanomaterials for fabricating electrochemical hydrogen peroxide sensors. *Biosens. Bioelectron.* 89 (Part 1): 249–268.

214 Li, Z., Xie, C., Wang, J. et al. (2015). Direct electrochemistry of cholesterol oxidase immobilized on chitosan–graphene and cholesterol sensing. *Sens. Actuators B Chem.* 208: 505–511.

215 Jiang, Z., Wang, J., Meng, L. et al. (2011). A highly efficient chemical sensor material for ethanol: Al_2O_3/graphene nanocomposites fabricated from graphene oxide. *Chem. Commun.* 47 (22): 6350–6352.

216 Vilela, D., Parmar, J., Zeng, Y. et al. (2016). Graphene-based microbots for toxic heavy metal removal and recovery from water. *Nano Lett.* 16 (4): 2860–2866.

217 Yang, K., Chen, B., and Zhu, L. (2015). Graphene-coated materials using silica particles as a framework for highly efficient removal of aromatic pollutants in water. *Sci. Rep.* 5 (February): 11641.

218 Kim, T., Lee, J.S., Lee, G. et al. (2016). Autonomous graphene vessel for suctioning and storing liquid body of spilled oil. *Sci. Rep.* 6: 22339. https://doi.org/10.1038/srep22339.

219 Ramirez Leyva, J.H., Hethnawi, A., Vitale, G., and Nassar, N.N. (2018). Magnetic nanostructured white graphene for oil spill and water cleaning. *Ind. Eng. Chem. Res.* 57 (39): 13065–13076. https://doi.org/10.1021/acs.iecr.8b02785.

220 Riaz, M.A., McKay, G., and Saleem, J. (2017). 3D graphene-based nanostructured materials as sorbents for cleaning oil spills and for the removal of dyes and miscellaneous pollutants present in water. *Environ. Sci. Pollut. Res.* 24 (36): 27731–27745. https://doi.org/10.1007/s11356-017-0606-x.

221 Neuberger, N., Adidharma, H., and Fan, M. (2018). Graphene: a review of applications in the petroleum industry. *J. Pet. Sci. Eng.* 167: 152–159. http://www.sciencedirect.com/science/article/pii/S0920410518303218.

222 Stanford, M.G., Li, J.T., Chen, Y. et al. (2019). Self-sterilizing laser-induced graphene bacterial air filter. *ACS Nano* 13 (10): 11912–11920. https://doi.org/10.1021/acsnano.9b05983.

223 Bong, J., Lim, T., Seo, K. et al. (2015). Dynamic graphene filters for selective gas-water-oil separation. *Sci. Rep.* 5 (1): 14321. https://doi.org/10.1038/srep14321.

224 Xiao, X., Wang, J., Liu, C. et al. (2006). In vitro and in vivo evaluation of ultra-nanocrystalline diamond for coating of implantable retinal microchips. *J. Biomed. Mater. Res. B Appl. Biomater.* 77 (2): 273–281.